

**A Genome-wide RNAi Screen for Modifiers of
Aggregates Formation by Mutant Huntingtin in
*Drosophila***

Sheng Zhang^{1, 2*}, Richard Binari^{1, 3}, Rui Zhou¹ and Norbert Perrimon^{1, 3*}

¹Department of Genetics and ³Howard Hughes Medical Institute

Harvard Medical School, Boston, MA 02115, USA

²Current address: Research Center for Neurodegenerative Diseases, the Brown
Foundation Institute of Molecular Medicine, the University of Texas Health
Science Center at Houston, Houston, TX 77030

**corresponding authors.*

Running title:

A *Drosophila* RNAi Screen for Aggregation Regulators

Key words:

protein mis-folding, aggregates formation, neurodegeneration, Huntingtin and Huntington's disease (HD), *Drosophila* genome-wide RNAi screen.

Corresponding authors:

Sheng Zhang^{1,2} and Norbert Perrimon^{1,3}

¹Department of Genetics and ³Howard Hughes Medical Institute
Harvard Medical School
77 Avenue Louis Pasteur
Boston, MA 02115, USA

Phone: (617) 432-7671
Fax: (617) 432-76888
Email: perrimon@receptor.med.harvard.edu

²Current address:
Research Center for Neurodegenerative Diseases
The Brown Foundation Institute of Molecular Medicine
The University of Texas Health Science Center at Houston
1825 Pressler Street
Houston, TX 77030

Phone: (713) 500-3493
Fax: (713) 500-2208
Email: sheng.zhang@uth.tmc.edu.

Abstract

Protein aggregates are a common pathological feature of most neurodegenerative diseases (NDs). Understanding their formation and regulation will help clarify their controversial roles in disease pathogenesis. To date there has been few systematic study of aggregates formation in *Drosophila*, a model organism that has been applied extensively in modelling NDs and screening for toxicity modifiers. We generated transgenic flies lines that express eGFP-tagged mutant Huntingtin (Htt) fragments with different length of polyglutamine (polyQ) tract, and showed that these Htt mutants develop protein aggregates in a polyQ-length and age-dependent manner in *Drosophila*. To identify central regulators of protein aggregation, we further generated stable *Drosophila* cell lines expressing these Htt mutants and also established a cell-based quantitative assay that allows automated measurement of aggregates within cells. We then performed a genome-wide RNA interference (RNAi) screen for regulators of mutant Htt aggregation and isolated 126 genes involved in diverse cellular processes. Interestingly, although our screen focused only on mutant Htt aggregation, several of the identified candidates were known previously as toxicity modifiers of NDs. Moreover, modulating the *in vivo* activity of *hsp110* (CG6603) or *tra1*, two hits from the screen, affect neurodegeneration in a dose-dependent manner in a *Drosophila* model of Huntington's disease (HD). Thus, other aggregates regulators isolated in our screen may identify additional genes involved in protein folding pathway and neurotoxicity.

Introduction

The presence of protein aggregates in the brains of patients has long been recognized as a common pathological feature of many neurodegenerative diseases, such as Alzheimer's, Parkinson's, Amyotrophic Lateral Sclerosis (ALS, Lou Gehrig's Disease) and polyglutamine (polyQ) diseases (BRUIJN *et al.* 2004; CAUGHEY and LANSBURY 2003; GUSELLA and MACDONALD 2002; PASINELLI and BROWN 2006; ROSS and POIRIER 2005; ROSEN *et al.* 1993; SISODIA 1998; SPILLANTINI *et al.* 1997). The close link between the diseases and aggregates is especially prominent among polyQ diseases, as best exemplified by Huntington's disease (HD). HD is caused by the expansion of a polyQ tract at the N-terminus of Huntingtin (Htt) protein (The Huntington's Disease Collaborative Research Group 1993). In human, the length of this polyQ tract is normally within the range of 7 to 26, whereas in HD patients it is invariably expanded to longer than 35 (The Huntington's Disease Collaborative Research Group, 1993; ANDREW *et al.* 1993; SNELL *et al.* 1993). One particularly intriguing pathological feature of HD is the presence of intracellular aggregates composed of processed N-terminal Htt (GUSELLA and MACDONALD 2002; ROSS and POIRIER 2005; SISODIA 1998). The intimate links between aggregates and HD are quite striking. In particular, genetic analyses revealed the existence of an inverse correlation between the length of the polyQ tract and the age of onset of the disease, while many *in vivo* and *in vitro* studies have demonstrated that mutant Htt containing longer glutamine tracts have an increasing propensity to form aggregates (PENNEY *et al.* 1997; SCHERZINGER *et al.* 1997). Similar relationships are also observed in eight other polyQ diseases such as spinocerebellar ataxias (SCAs)(GUSELLA and MACDONALD 2002; ROSS and POIRIER 2005; SISODIA 1998). Because of this intimate link, aggregates have been suspected as the cause of neural toxicity. However, other studies found no correlation between

the distribution of aggregates in the brain and neurodegeneration, and proposed that aggregates are simply byproducts of the disease process. Still other studies have argued that aggregates play a beneficial role by sequestering toxic species within the cell (CAUGHEY and LANSBURY 2003; GUSELLA and MACDONALD 2002; ROSS and POIRIER 2005; SISODIA 1998). Noticeably, a recent study following aggregates formation in cultured neurons proposed that aggregates formation reduces the levels of diffusive mutant Htt and protects against its toxicity (ARRASATE *et al.* 2004).

Drosophila has been an excellent model system to study various NDs, as toxicity of these disease proteins can often be well-recapitulated in the fly (BILEN and BONINI 2005; MARSH and THOMPSON 2006). Because of this, *Drosophila* has been widely used to screen for toxicity modifiers of different disease proteins, especially for polyQ diseases, and a diverse group of toxicity modifiers with functions in different cellular processes have been isolated, such as protein folding (*e.g.*, *dnaj1* and *tpr2*) (CHAN *et al.* 2000; KAZEMI-ESFARJANI and BENZER 2000), ubiquitin modification and protein degradation (*e.g.*, *smt3* and *uba2*) (CHAN *et al.* 2002; STEFFAN *et al.* 2004), transcriptional regulation (*e.g.*, *sin3* and *rpd3*) (FERNANDEZ-FUNEZ *et al.* 2000; STEFFAN *et al.* 2001) and others (CHEN *et al.* 2003; COOPER *et al.* 2006; KANUKA *et al.* 2003; RAVIKUMAR *et al.* 2004; SHULMAN and FEANY 2003; WU 2005). Notably, when tested in *Drosophila*, a human chaperone Hsp70 and a *Drosophila* co-chaperone *dhdj1* (also known as *Hsp40* or *dnaj1*) can significantly suppress polyQ toxicity and also alter the solubility of aggregates, suggesting a possible correlation between aggregates and neurotoxicity (CHAN *et al.* 2000; WARRICK *et al.* 1999).

Although *Drosophila* has been successfully used to identify toxicity modifiers, no comprehensive analysis of regulators of aggregates formation has

been conducted, probably due to a lack of simpler assay to assess the aggregates formed *in vivo*. To systematically identify central regulators of protein aggregation in this model organism, we focused on the well-studied HD protein Htt. Earlier studies in different model system have already demonstrated that expression of mutant Htt or other polyQ disease proteins induces polyQ length-dependent neurodegeneration (BILEN and BONINI 2005; GUSELLA and MACDONALD 2002; MARSH and THOMPSON 2006). To evaluate the aggregates formation by mutated Htt in *Drosophila*, we first generated transformant lines for eGFP-tagged Htt exon 1 fragments containing different length of glutamine repeats and analyzed their ability to form aggregates in *Drosophila* tissues. We then established a cell-based quantitative assay that allows automated measurement of aggregates within cells by combining automated microscopy with quantitative analysis. Using this automated protocol, we performed a high-throughput genome-wide RNA interference (RNAi) screen in *Drosophila* cells and identified a diverse group of genes that can affect formation of aggregates by mutant Htt.

Results

Htt mutants form aggregates in a polyQ length- and age-dependent manner in *Drosophila* tissues

In order to screen for regulators of aggregates formation, we first needed to select a mutant disease protein whose propensity to form aggregates could be modulated by the cellular genetic environment. Htt mutants are ideal candidates for this purpose, given the unique feature of a correlation between their propensity to form aggregates and the length of their polyQ tracts (GUSELLA and MACDONALD 2002; SCHERZINGER *et al.* 1997). Accordingly, we

focused our study on the well-established Htt constructs with Htt exon1 (Httex1) containing different lengths of the polyQ tract: Httex1 with 25 glutamines (Q25) that represents wild-type Htt control, and mutated Htt containing an increasing length of glutamine repeats: 46Q, 72Q and 103Q (simplified in the following text as Httex1-Q25, Q46, Q72 and Q103) (KAZANTSEV *et al.* 1999). These Httex 1 proteins, which are tagged at their C-termini with eGFP, have been previously shown to form visible polyQ length-dependent aggregates in cultured mammalian cells (KAZANTSEV *et al.* 1999). We cloned this set of eGFP-Httex1 constructs into the pUAST vector and generated corresponding transgenic fly lines, which allow the targeted expression of Httex1 transgenes in selected tissues using the Gal4 binary expression system (Fig. 1A) (BRAND and PERRIMON 1993).

We then examined the aggregation property of these Httex1 proteins in several *Drosophila* tissues. Remarkably, when expressed in the eye using the eye-specific GMR-Gal4 driver, the aggregation patterns of the eGFP-tagged Httex1 proteins can be conveniently monitored directly in adult fly eyes under the fluorescence microscopy (Fig. 1B-K). For example, while Httex1-Q25 maintains a diffuse cytoplasmic distribution over the life of the fly (Fig. 1C,D), Httex1-Q103 exists almost exclusively in prominent aggregates soon after it is expressed and are already prominent in newly hatched adults (Fig. 1J, K and data not shown). Further, while the expression of both Httex1-Q46 and -Q72 is diffuse in young flies, aggregates gradually develop as the flies age, with Q72 forming aggregates at a faster rate than Q46 (Fig. 1E-I).

We next analyzed aggregates formation by these Httex1 proteins in the fly central nervous system (CNS). When expressed in all neuronal cells using the pan-neuronal Elav-Gal4 driver, these Httex1 proteins showed similar

aggregation patterns as in the eye (Fig. 1L-P and data not shown). Noticeably, again among the tested Httex1 proteins, the age-dependent nature of aggregates formation was most clearly exemplified in flies expressing Httex1-Q46. As shown by confocal imaging, in 2-day-old adult flies, Httex1-Q46-eGFP protein was evenly distributed in the brain (Fig. 1L, N). However, by day 30, predominant eGFP-positive aggregates were present throughout the brain (Fig. 1M, O). Thus, consistent with the observations in mammalian cells, these Htt exon1 proteins show both age- and polyQ length-dependent patterns of aggregates formation in *Drosophila* tissues.

An important biochemical definition of protein aggregates is their resistance to detergent SDS, which can be detected on Western blot as SDS-insoluble large protein complexes that are retained in the stacking gel. To confirm that the observed bright eGFP-positive puncta in *Drosophila* tissues are indeed protein aggregates, we extracted whole proteins from adult fly heads at different ages and performed Western analysis. As shown in Fig. 1P, SDS-resistant large protein complexes were absent in aged 30-day-old control flies expressing eGFP alone or eGFP-tagged wildtype Httex1-Q25; they were present in both young (2-day-old) and aged (30-day-old) Httex1-Q72 and Httex1-Q103 flies; most tellingly, these complexes were absent in young (2-day-old) but were clearly present in aged (30-day-old) Httex1-Q46 flies (lanes 3 and 4 in Fig. 1P, highlighted with blue dashed lines), mirroring the appearance of eGFP-positive puncta in these animals. Thus, the development of SDS-insoluble large protein complexes, a process that is also both polyQ length- and age-dependent, correlates with the appearance of eGFP-positive puncta in the fly tissues, supporting that these fluorescent puncta are indeed protein aggregates.

In addition to aggregates formation, we also observed the expected, polyQ length-dependent toxic effect of these mutant Httex1 proteins, that is, Httex1 with longer polyQ tract causes more severe degenerative phenotypes, such as reduced survival rate during development, as well as progressive eye degeneration, declining mobility and shortened life-span in adults (arrows in Fig. 1K and data not shown). Together, these results demonstrated that both the formation of aggregates and the toxicity of mutant Htt could be recapitulated in *Drosophila* expressing eGFP-tagged Htt-exon1-Qn reporters. Further, among the tested Httex1 proteins, the progressive nature of aggregates development was most clearly exhibited by Httex1-Q46-expressing animals, suggesting that it might be more susceptible to modulations by other cellular factors and thus represents a good candidate as a reporter in screens for regulators of aggregates formation.

An imaging-based, high-throughput assay for aggregates formation in *Drosophila* cells

With the recent advent of RNAi technology and the development of genome-wide dsRNA libraries, it is possible to quickly and systematically evaluate all known genes in a model organism for their effects on a studied question. In *Drosophila*, RNAi-mediated gene knockdown is especially efficient in cultured cells and genome-wide RNAi screens have been well developed and applied to exploring multiple signalling (CAPLEN *et al.* 2000; CLEMENS *et al.* 2000; FRIEDMAN and PERRIMON 2007). To establish a relevant cell-based assay suitable for an RNAi screen for aggregation regulators in *Drosophila*, we choose hemocyte-like S2 and neuronal-like BG2 cells and generated stably transformed

cell lines in which the expression of the above eGFP-tagged Httex1 proteins is controlled by the copper-inducible *metallothionein* promoter (Fig. 2A). Consistent with the *in vivo* results, in both of these two cell lines, these Httex1 proteins showed similar behaviour of polyQ length-dependent aggregation (Fig. 2B and data not shown). Importantly, aggregates in these cells emit intense fluorescent signals that are easily identifiable even when viewed at low-magnification, making it feasible to use the image-based approach to screen for aggregates regulators.

To adopt such an image-based assay for a high-throughput screen, it is important that individual aggregates and each cell can be clearly distinguishable to ensure reliable quantification. We found that under the cultured condition, neuronal-like BG2 cells more easily congregate together and form clumps even before reaching confluence, impeding the clear visualization and quantification of both the aggregates and cell number (data not shown), while such issues are much less prominent in S2 cells, which are more prone to spread out and form a single layer over the surface before reaching confluence (Fig. 2B). Moreover, in the established S2 cell line expressing Httex1-Q46-eGFP, aggregates develop in approximately 50% of the cells, ideal for a modifier screen to identify both suppressors and enhancers of mutant Htt aggregation (Fig. 2B). Accordingly, we choose this S2 cell line expressing Httex1-Q46-eGFP for the ensuing RNAi screen.

To demonstrate the relevance and sensitivity of this cell-based system for a modifier screen, we treated these cells with a dsRNA against *dhdj1*, a known suppressor of aggregates (CHAN *et al.* 2000; KAZEMI-ESFARJANI and BENZER 2000), and found that it significantly enhanced aggregates formation

(Fig. 3C); conversely, treatment with dsRNA targeting the eGFP tag in the Httex1-Q46 reporter completely abolished fluorescent signals (Fig. 3D).

To ensure that this cell-based assay could be applied to a high-throughput screen, we further developed an automated assay protocol. Using this protocol, sample images were captured by an automated microscope, with aggregates revealed by their prominent eGFP signals and individual cells by DAPI nuclear staining. Details about the aggregates (*i.e.*, the size, total number and signal intensity of aggregates) and the number of cells in the imaged fields were automatically quantified using the MetaMorph analytic software. Since the aggregates are highly enriched with eGFP-tagged mutant Htt (Httex1-Q46-eGFP), the level of fluorescent signal from the aggregates is significantly higher than that from the cytoplasm and from background noise, thus allowing their clear identification and quantification. As seen in Fig.2C, this automated quantification gave rise to satisfactory accuracy in measuring both the aggregates and cell number (see legends for Fig. 2C and Materials and Methods for details).

When evaluated by such a quantitative approach, most dsRNAs tested show no effect on aggregates formation, while dsRNA specifically directed against *dhdj1* as a positive control significantly enhanced aggregates formation and *dhdj1* was reproducibly categorized as a strong suppressor (Fig. 3C). Furthermore, comparison between duplicate experiments reveals that overall both the assay and the quantification results are highly reproducible (Fig. 2D & data not shown).

Genome-wide RNAi screens for regulators of aggregates formation

Primary screens After optimization of this cell-based assay in a 384-well plate format, we performed an RNAi screen in duplicate using a *Drosophila* genome-wide library of ~24,000 dsRNAs (BOUTROS *et al.* 2004), with the effect of each dsRNA on aggregates formation quantified based on three parameters: the average number, size and signal intensity of aggregates (Figs. 2D and S1). For each plate, the average value and standard deviation (SD) for these three parameters from whole-plate samples were also calculated. For a dsRNA-treated sample in the primary screen, if the value of any of the three parameters was greater than 2xSD of the whole-plate average, it was considered to have a significant effect on aggregates formation and was selected as a potential candidate (Figs. 2D and 2E, also see Materials and Methods for screen details). Based on the above selection criterion, we identified 644 candidate dsRNAs from the primary screens that potentially enhance or suppress aggregates formation.

Secondary Assays To eliminate false positives resulting from indirect effects on aggregates formation, we further evaluated the 644 candidate dsRNAs from the primary screen in the following steps (Figs. 2E and S2, see legends and Materials and Methods for details): (1) removed dsRNA amplicons that contain 21-bp overlaps with more than 5 other genes in the genome, which are expected to cause a significant non-specific off-target RNAi effects (KULKARNI *et al.* 2006; MA *et al.* 2006); (2) removed those that are known to function in general protein synthesis (*e.g.*, cytoplasmic or mitochondrial ribosomal proteins), which affect overall protein synthesis within the cell, indirectly affecting the formation of aggregates that depends upon the amount of available mis-folded Htt protein (SCHERZINGER *et al.* 1999); (3) removed those that failed to reproduce their effect on aggregation in an intermediate screen using the re-synthesized dsRNAs; (4) identified and removed candidates that

affect the activity of *metallothionein* promoter in a luciferase-based assay (*e.g.*, COP complex components and the copper transporter); (5) validated each remaining hit by synthesizing and re-testing one or two more dsRNAs targeting different regions of the candidate gene. Genes that failed to repeat their effect on modulating aggregation in these additional rounds of testing were removed from consideration. In total, 126 genes passed both the primary screens and all subsequent validation steps (Figs. 2E and S2).

Functional categorization of regulators of aggregates formation identified by the screen

Of the 126 validated regulators from the screen, 52 act as enhancers and 74 as suppressors of aggregates formation (Fig. 4A-C and Table 1. See Supplementary Tables S1 and S2 for list of these genes and associated information). Please *note* that throughout this study, “Suppressor” is defined genetically as a candidate that causes an increased formation of aggregates after dsRNA-mediated knockdown of the corresponding gene, and *visa versa*, “Enhancer” is similarly defined as the one that lead to a decreased formation of aggregates in the assay. Examples of some of these modifiers are shown in Figure 3. Interestingly, although overall only 50% of fly genes are conserved in humans (RUBIN *et al.* 2000), 71% (90 of 126) of isolated candidates have predicted human orthologues, with 25 of them encoding proteins that have been implicated in human diseases (See Table S2).

Based on their predicted function, these 126 genes can be further categorized into different classes, the largest category of which contains genes that function mainly in protein biogenesis (Fig. 4A, and Table 1). Interestingly,

the major classes of suppressors from a *C. elegans* screen in the muscle tissue for modifiers of polyQ aggregation are also involved in protein biogenesis, which have been proposed to represent the “protein homeostatic buffer” that can respond to and prevent the aggregation of mis-folded proteins (MORIMOTO 2008; NOLLEN *et al.* 2004).

In addition, all 14 genes in the cytoskeleton/protein trafficking group were isolated as enhancers of aggregation, suggesting that formation of visible aggregates might involve active transport to concentrate mis-folded proteins into a specific compartment within the cell (GARCIA-MATA *et al.* 1999), while interference with cytoskeleton integrity or the protein transport machinery might disrupt such a process.

In eukaryotes, multiple families of chaperones with diverse cellular functions are present (BUKAU *et al.* 2006; CRAIG *et al.* 1994; WHITESELL and LINDQUIST 2005). Within the cell, chaperones are essential in facilitating the proper folding of newly-synthesized proteins and the re-folding of mis-folded proteins to maintain them in their soluble native state (BUKAU *et al.* 2006; CRAIG *et al.* 1994; WHITESELL and LINDQUIST 2005). Since the aggregates in this assay were derived from mis-folded mutant Htt, it is expected that chaperones play a central role in regulating aggregates formation. Indeed, another major class of modifiers from the screen includes several chaperones and their regulatory proteins, such as the chaperone proteins *CG6603* (a member of Hsp110 subfamily chaperones, see below), *hsp83* (Hsp90 family) and *hsc70-5* (Hsp70 family), the co-chaperone *dhdj1* (Hsp40 family), chaperonin *T-cp1* and the heat shock transcription factor *hsf*. *Hsf* is activated in response to heat-shock and

other cellular stresses to induce the expression of downstream chaperone proteins (CRAIG *et al.* 1994). Knockdown of all these chaperone genes enhanced aggregates formation (*i.e.*, suppressors), while depletion of *CG6603* gave rise to the strongest enhancing effect of all the regulators isolated (Figs. 3B & 3C, also see below). Surprisingly, knockdown of *hsc70-3* and *hsc70-4*, two abundant Hsp70 chaperones, both caused reduction of aggregates formation. Previous studies suggest that each chaperone has selective substrate preferences, and chaperones further show specificity in modulating polyQ neurotoxicity (CHAN *et al.* 2000). In addition, some chaperones are known to be involved in essential cellular processes. For example, *hsc70-4* in *Drosophila* is critical for clathrin-dependent endocytosis (CHANG *et al.* 2004; CHANG *et al.* 2002). Thus, modulating the activities of these chaperones might indirectly affect the aggregates formation, and their observed differential effect on aggregation could be due to their distinctive cellular functions and substrate specificity.

Moreover, a dozen modifiers, such as *uba1*, *smt3* and *lwr*, are involved in ubiquitin- or sumo-modification and protein degradation pathways, supporting that clearance of mis-folded proteins by the cellular degradation machinery serves as an important regulatory step in aggregates formation.

Noticeably, several components of the nonsense-mediated mRNA decay (NMD) pathway were isolated, which all acted as suppressors of aggregates formation. NMD is a cellular surveillance machinery that promotes the degradation of abnormal mRNAs containing premature termination codons (VALENCIA-SANCHEZ and MAQUAT 2004). The potential mechanism for the NMD

pathway in modulating aggregation formation is not clear. Interestingly, one central component of the NMD complex, *smg1*, encodes a large protein with a PI3,4-kinase domain, a HEAT domain and, notably, a heat-shock protein Hsp70-like domain (GATFIELD *et al.* 2003). This raises the possibility that the NMD pathway also has some functional overlap with the chaperone machinery, and as such, senses and modulates the formation of aggregates through its crosstalk with chaperones. Alternatively, since NMD acts by promoting the decay of abnormal mRNAs, another attractive possibility is that it recognizes the expanded CAG repeats in the mRNA transcripts of mutant Htt and promotes their degradation (VALENCIA-SANCHEZ and MAQUAT 2004).

A number of kinases and phosphatases signalling genes were also isolated from the screen, including a PI-3,4 kinase PI3K68D, the alpha and beta subunits of casein kinase II (CKII), as well as phosphatases *CG1906* and *spaghetti*. *CG1906* encodes a phosphatase 2C-like protein, while *spaghetti* encodes a TPR-containing protein with serine/threonine phosphatase activity. The exact role of these signalling molecules in modulating aggregates formation remains to be clarified. Noticeably, *spaghetti* was reported to interact with chaperone Hsp90, another aggregates regulator isolated from the screen, and normally forms a large chaperone complex (MARHOLD 2000). This raises the possibility that *spaghetti* affects aggregates formation by regulating the activity of chaperones within the cell. It is not clear if these kinases and phosphatases function together and converge on the same pathway (such as the chaperones), or exert their effect through separate pathways. As kinases and phosphatases provide targets of choice in drug design, it is of interest to identify the exact

pathway(s) regulated by these signalling molecules to decipher how they influence aggregates formation.

Another potential class of modifiers, including *jra1*, *raw*, *tao1*, *cka* and *lic*, is involved in Jun-N-terminal Kinase (JNK) signalling. The presence of aggregates within the cell might trigger a cellular stress/defense response, which is normally mediated by the JNK signalling pathway (WESTON and DAVIS 2002).

We also noticed that although our screen focused on identifying regulators of aggregates formation, a number of isolated candidates from the screen have been previously identified as toxicity modifiers for polyQ or other aggregates-associated diseases (Table 2). For example, *smt3* and *uba 2*, which encode SUMO protein and SUMO-activating enzyme, respectively, have been shown previously to modulate polyQ pathogenesis in *Drosophila* (CHAN *et al.* 2002; STEFFAN *et al.* 2004), and both were isolated in our screen as aggregation enhancers. Similarly, *sin3A* and *rpd3*, which are components of the Sin3 chromatin remodeling complex involved in transcriptional repression, previously characterized as modifiers of polyQ toxicity (FERNANDEZ-FUNEZ *et al.* 2000; STEFFAN *et al.* 2001), were identified in our screen as aggregation suppressors. In addition, *tao1* has been reported to be involved in tauopathy and *rab1* to be associated with α -Synuclein-induced toxicity (COOPER *et al.* 2006; SHULMAN and FEANY 2003). It is possible that the mechanisms by which these genes modulate neurodegeneration are completely separable from their role in regulating aggregates formation. For example, it has been suggested that through the SUMO modification of Htt, *smt3* and *uba2* might modulate cellular

toxicity by affecting Htt's transcriptional repression activity or its subcellular localization (CHAN *et al.* 2002; STEFFAN *et al.* 2004). Nevertheless, the observation of an overlap between these two groups of modifiers raises a possibility that the effects of these modifiers on aggregates formation also contributes to their role in modulating neuronal toxicity.

Hsp110 as a potent suppressor of aggregates formation and neurotoxicity

CG6603 was isolated as the most potent aggregates suppressor from the screen: RNAi-mediated depletion of CG6603 caused formation of prominent aggregates in almost 100% of dsRNA-treated cells (Fig. 3B), and quantification analyses of the three evaluation parameters all showed that CG6603 is the most potent suppressor of aggregates formation identified in our screen (Fig. 2D), suggesting it might play an important role in regulating the aggregation of mutant Htt protein. Because of this, we further examined its role during development and in neurodegeneration.

The CG6603 gene in *Drosophila* has not yet been extensively studied. Several mutant alleles of CG6603 exist, all of which cause early lethality when homozygous. By mosaic clonal analyses, we further found that patches of CG6603 mutant tissue failed to develop, indicating that the gene encodes an essential cellular function (data not shown). Further, overexpression of wild-type CG6603 caused a toxicity effect in the targeted tissues (Fig. S3). Together, these results indicate that an optimal level of CG6603 activity is essential for normal animal development.

To study the role of CG6603 in neurodegeneration, we next tested its genetic interaction with HD93 (*Httex1p-93Q*), a well-characterized *Drosophila* HD model (STEFFAN *et al.* 2001). In HD93 flies, a mutant Htt containing a polyQ tract of 93 residues is ectopically expressed in the *Drosophila* eye, causing an age-dependent degeneration. At day 7, the degeneration is manifested exteriorly by the clear de-pigmentation in the posterior region of the eye (compare Figs. 5B with 5A); as the fly ages this degeneration gradually spreads to the whole eye (compare Figs. 5E with 5B). When tested in HD93 flies, CG6603 showed a strong dosage-dependent modifying effect on neurodegeneration: in flies heterozygous for mutations in CG6603, which halved the endogenous dosage of the corresponding protein, eye degeneration was significantly accelerated (Fig. 5C). Further, increasing the endogenous level of wild-type CG6603 by ectopically expressing low levels of CG6603 noticeably suppressed eye degeneration in HD93 flies (Fig. 5F, see Fig. S3 for additional controls for this assay).

CG6603 encodes a protein of 804 amino acids with significant sequence homology to the Hsp110 subfamily of chaperones, which is distinguished from other Hsp70 family chaperones by its unusually large size (EASTON *et al.* 2000). Currently, alleles of CG6603 have been referred to as Hsc70Cb, solely due to its cytological location at polytene band 70C. To avoid confusion with the general Hsp70 proteins, we refer to it as dHsp110 in this study. Consistence with our result, that Hsp110 was the most potent suppressor of aggregates formation by mutant Htt, a previous study showed that mammalian Hsp110 conferred cellular thermo-resistance in cultured cells and was several-fold more efficient than Hsc70 in preventing aggregation of denatured luciferase (OH *et al.* 1997). Thus, together with the observation of its dosage-dependent genetic

interaction with HD flies, Hsp110, a strong aggregation suppressor, might also be a potent suppressor of mutant polyQ-induced neurodegeneration.

tra1* modulates the toxicity of mutant Htt *in vivo

In addition to *dhsp110*, we found that two mutant alleles of *tra1* (also called *Nipped-A*), another aggregation suppressor identified from the screen, also showed a dosage-dependent modifying effect on neurotoxicity of mutant Htt: in a heterozygous *tra1* mutant background, the eye degeneration of HD93 flies was significantly enhanced (Fig. 5D), suggesting a role of *tra1* in mutant Htt-induced neurotoxicity. Similar to *hsp110*, knockdown of *tra1* significantly increased aggregates formation in the assay. *tra1* is believed to function in the SAGA complex to regulate transcription. It encodes a large protein containing a HEAT domain, a PI-3,4 kinase-like domain and a TPR repeat. The role of *tra1* in regulating aggregates formation remains to be clarified.

Discussion

A genome-wide RNAi screen for regulators of aggregates formation in *Drosophila* cells

In *Drosophila*, which has been extensively used to study polyQ and other neurodegenerative diseases, most of the previous studies focused on toxicity; no systematic analysis of regulators of aggregates formation has been carried out in this system. By developing a cell-based quantitative assay and using a genome-wide collection of dsRNAs in *Drosophila*, we performed a high-throughput RNAi screen and identified over one hundred aggregation regulators. Clearly more studies are needed to further validate the identified candidates and investigate the exact mechanisms by which these regulators

modulate aggregation. Nevertheless, this genome-wide RNAi screen should help complement the previous studies focusing on toxicity in neurodegenerative diseases. For example, by comparing hits from our screen with previously identified toxicity modifiers in *Drosophila*, we found an interesting overlap between these two groups of genes. In addition, we showed that *Drosophila hsp110* (CG6603) and *tra1* can both modify neurodegeneration of HD flies in a dosage-dependent manner. Together, they support that modulating aggregates formation might have therapeutical implications in treating neurodegenerative diseases.

In addition, it is conceivable that this imaging-based high-throughput screen approach, which combines automated microscopy with quantitative analysis, could be adopted as an alternative, easily-applicable format for studying other aggregates-associated diseases.

Hsp110 chaperone as a potent suppressor of aggregates formation and neurotoxicity

From the screen, *hsp110* (CG6603) stands out as the most potent suppressor of aggregates formation. By further characterizing its mutant phenotypes, we found that an optimal level of CG6603 activity is essential for normal animal development, as both loss of its endogenous function and high-level overexpression were detrimental to the animal. Moreover, CG6603 modulates neurodegeneration of HD flies in a dosage-dependent manner. Together, these data suggest a unique role for CG6603 in regulating normal animal development, protein folding and neurotoxicity.

Noticeably, in COS-7 cells, over-expression of the Hsp110 family member Hsp105 α suppresses both the aggregation and cellular toxicity of mutated androgen receptor, the causative gene for the polyQ disease SBMA (spinalbulbar muscular atrophy) (ISHIHARA *et al.* 2003). In addition, a Hsp110 homologue in *C. elegans* has recently been identified as a strong suppressor of aggregates formation by ALS-associated mutant SOD1 (see below), and more interestingly, in a mouse ALS model, three Hsp110 family members were found to physically associated with mutant but not wildtype SOD1 as animals age (WANG *et al.* 2009a; WANG *et al.* 2009b). Together, these results suggest a conserved role of Hsp110 family chaperones in modulating misfolding and toxicity of mutant disease proteins.

Despite being highly conserved from yeast to human, being one of the most abundant proteins in the mammalian brain and much more effective than Hsc70 in preventing aggregation of denatured protein, there are only limited functional studies on Hsp110 family of proteins and their exact biochemical function remain not clear (EASTON *et al.* 2000; OH *et al.* 1997; OH *et al.* 1999; SHANER *et al.* 2005; YAM *et al.* 2005). It has been suggested that Hsp110 cannot on its own re-fold a denatured protein, but instead functions as a “holdase” by binding and maintaining the denatured protein in a soluble folding-competent state, and subsequently cooperating with other Hsp70 chaperones for re-folding (OH *et al.* 1997; OH *et al.* 1999; SHANER *et al.* 2005; YAM *et al.* 2005). More recently, Hsp110 proteins were also suggested to act as nucleotide exchange factors for general Hsp70 chaperones (DRAGOVIC *et al.* 2006; POLIER *et al.* 2008; RAVIOL *et al.* 2006; SCHUERMANN *et al.* 2008). Interestingly, although multiple families of chaperone proteins exist in eukaryotes, Hsp110 showed the strongest effect as an aggregates suppressor in the screen (Figs. 3B, 3C and data not shown). Chaperones function in diverse cellular processes, but each

chaperone has a selective substrate preference (BUKAU *et al.* 2006). In addition, chaperones display specificity in modulating polyQ neurotoxicity (CHAN *et al.* 2000). Thus, given the dosage-sensitive effect of Hsp110 in normal *Drosophila* development and in modulating Htt toxicity, it is possible that Hsp110 plays a rate-limiting, regulatory role for general Hsp70 chaperones, a role similar to that of Hsp40 which acts as a co-chaperone for Hsp70 chaperones by stimulating their ATPase activity (BUKAU *et al.* 2006; CRAIG *et al.* 1994). Alternatively, Hsp110 might be the main chaperone that is more specific for the proper folding of mutant polyQ proteins. The detailed mechanism of action of Hsp110 proteins remains to be clarified. Nevertheless, results from our RNAi screen and genetic analyses, together with previous studies, suggest that Hsp110 chaperones play an important role in regulating the proper folding and toxicity of mutant Htt.

Comparison with aggregation regulators isolated from other large-scale RNAi screens in model organisms

Recently, several large-scale RNAi-based screens in *C. elegans* for aggregation regulators of different NDs-associated proteins have been reported. We thus compared our candidates with that from these studies.

A total of 186 suppressors were isolated from a genome-wide RNAi screen for genes regulating polyQ aggregation in *C. elegans*, and knock-down of these genes by dsRNA promote aggregates formation in muscles expressed a threshold-length polyQ protein (Q35-YFP) (NOLLEN *et al.* 2004). Comparison of the results of these two screens reveals many overlapping hits, including *hsf*, *Hsc70-5*, *uba1*, *T-cp1* and *rab1*, as detailed in Supplemental file Table-S3.

However, we also noted significant differences between the results of the two screens. For example, on one hand, knockdown of *rme-8* gene, a DnaJ domain chaperone protein, could enhance aggregates formation in *C. elegans*, while its closest homolog in *Drosophila*, *Rme-8*, showed no effect in our study. On the other hand, the fly *dhdj1* gene (also called *hsp40* and *dnaj1*), which encodes a DnaJ domain protein of Hsp40 co-chaperone family, showed strong effect in our study (Fig. 3C) while its closest homolog in the worm, *dnaj-13*, was not found in the *C. elegans* study. In addition, many regulators from our study were not identified in the *C. elegans* screen, such as *hsp110*, *JNK* members and the *NMD* pathway, and *visa versa*. Most intriguingly, there are many cases where the same group of genes isolated from these two screens elicit different responses in the two systems, such as *rab1* and *Tbp-1*, as down regulation of these genes' expression led to an increased aggregates formation in the *C. elegans* study but an opposite effect in our study (Table-S3). Among such genes, perhaps the most obvious examples are those involved in protein biogenesis. In the *C. elegans* screen, 40 identified suppressors were ribosomal proteins, and their depletion by RNAi promoted premature formation of aggregates in the muscle (NOLLEN *et al.* 2004). In our study, 97 cytoplasmic and mitochondrial ribosomal proteins were also isolated from the primary screen. However, knockdown of these ribosomal proteins in the assay all significantly diminished aggregates formation in *Drosophila* cells (see Table-S3, Fig. S2 and Supplementary Information). Because formation of aggregates is sensitive to the level of Htt mutant expression (SCHERZINGER *et al.* 1999), and ribosomal proteins are involved in general protein synthesis, we suspect that the effect of these ribosomal proteins in our assay is likely to be indirect and thus removed from the follow-up studies. The reason(s) behind the differences between these two screens is still not clear, but likely due to many factors, such as an intrinsic

specie difference between the fly and the worm, different assay approaches (visual inspection of whole animals vs. computer imaging of cultured cells), or differential sensitivity of the experimental system (muscle tissue in *C. elegans* vs. *Drosophila* S2 cell lines). However, one important element might be that, compared with the cell-based assay that mainly reflect autonomous cellular effect, *C. elegans* as a complicated multi-cellular organism can integrate the sensing and responses to the aggregates-induced stress within a specific tissue (e.g., the muscle) at the whole animal-level, eliciting both autonomous and more-complicated non-autonomous responses (PRAHLAD and MORIMOTO 2009). Indeed, one recent study suggested that thermosensory neurons regulate the cellular heat-shock response in *C. elegans* (PRAHLAD *et al.* 2008). Further investigations will be needed to address these different observations. Nevertheless, hits from these two screens should complement each other, as they provide a valuable comparison that can broaden our understanding of regulation of aggregates formation in different experimental systems.

A major component of the Lewy bodies (LB) inclusions in Parkinson's disease (PD) is α -Synuclein (α -Syn) (SPILLANTINI *et al.* 1997). In two similar RNAi screens in *C. elegans*, one genome-wide and the other targeting 868 candidates, 84 and 20 hits, respectively, were identified that when knocked down, increased aggregation of fluorescence-tagged human α -Syn expressed in the worm body-wall muscles (HAMAMICHI *et al.* 2008; VAN HAM *et al.* 2008). Comparison of our result with these two studies revealed only limited overlaps: in both cases a chaperone protein Hsp83 or Dnaj-1 (Hsp40) (Tables S4 and S5).

Mutations in human superoxide dismutase (SOD1) gene are associated with ALS (BRUIJN *et al.* 2004; PASINELLI and BROWN 2006; ROSEN *et*

al. 1993). A whole-genome RNAi screen in *C. elegans* identified 81 suppressors, which when knocked down by RNAi increased aggregates formation in neurons expressing the YFP-tagged misfolding-prone SOD1 (G85R) mutant (WANG *et al.* 2009a). Interestingly, homologues of eight of these hits were also identified in our study, including *hsf*, *hsp110* and *rab11*, with another four among the candidates from our primary screen (Table S6). Again we noticed several cases where two homologous genes elicit opposite responses in the two screens (*e.g.*, *uba2* and *rab11*, see Table S6). We hypothesize that as in the above polyQ study, similar factors might be accountable for such opposite responses in this SOD1 screen as well. Nevertheless, the observation of more overlapping hits among polyQ, Htt (a polyQ disease) and SOD1 mutants than with α -Syn raises an intriguing possibility that polyQ and SOD1 mutants share more similarities in their aggregation processes than with α -Syn.

Note: While the manuscript for this study was being prepared, a RNAi screen similar to this study was reported by Doumanis *et al.*, who used a Httex1-62Q-eGFP reporter in *Drosophila* BG2 cells and identified 21 regulators after testing 7,200 *Drosophila* genes (DOUMANIS *et al.* 2009). Comparing the results from the two screens revealed several similarities (Table S7). First, 3 identical genes were isolated from both two screens: *sec23*, *deflated* (*defl*) and *CG4738* (Table S7). Importantly, these 3 genes showed similar effects on aggregation in both screens: knocking down of *sec23* and *CG4738* decreased aggregates formation, while reducing the level of *defl* increased aggregates formation. In addition, another 6 genes from the Doumanis *et al.* study were among the original 644 candidates from our primary screens, which were eventually removed from our final hit list after failing to pass the 2nd screens. These six genes also showed similar effects on aggregates formation in both

studies (Table S7). Moreover, we noticed that although Nup154, one of the hits from the Doumanis et al. study, was not identified in our screen, several other Nup family proteins, including Nup62, Nup98, Nup170 and Nup 358, were isolated from our study. The remaining differences between the results of the two studies are likely due to different selection criteria as well as different RNAi libraries and cell types used in the screens. It is highly likely that due to unavoidable variations in the experiments, extra false positives are included and extra false negatives are removed from both studies. Additional analyses are warranted to examine the identified regulators from these studies. Nevertheless, the significant overlap of the hits from these two independent screens support the reproducibility of the image-based RNAi screen for studying regulations of aggregates formation. Further studies will be needed to validate the *in vivo* effects of the identified candidates from these screens and uncover the mechanisms underlying their regulations.

Materials and Methods

DNA plasmids. DNA containing the mutant Httex1-Qn-eGFP variants (Q25, Q46, Q72 and Q103) were generously provided by the Hereditary Disease Foundation (HDF) (originally from Dr. A. Kazantsev (KAZANTSEV *et al.* 1999)) and cloned into the hygromycin-resistance pMK33 vector which contains the copper-inducible *metallothionein* promoter. See Supplemental Information for details about the plasmids and cloning procedures.

RNAi screen

Using a MultiDrop liquid dispenser, stable Httexon1-Qp47-eGFP cells were

aliquoted uniformly into 384-well dsRNA-containing plates at approximately 1×10^4 pMK33-Httex1-Qp46eGFP cells per well in 20 μ l of serum-free medium. After incubation at room temperature for 1 hour, 20 μ l of medium containing 10% fetal bovine serum (FBS; JRH Biosciences) was added. After 3 days of incubation, 25 μ l of medium containing CuSO_4 and 5% FBS was added to each well to reach a final copper concentration of 400 μ M to induce the expression of the Httex1-Qp46-eGFP reporter. After induction for another 2 days, cells were fixed using 4% formaldehyde at room temperature for 20 minutes. For cell staining, the samples were washed 3 times with PBST (1xPBS plus 0.1% Triton-X100) after fixation, then incubated with DAPI (0.2 μ g/ml final concentration, Molecular Probe) and Tritc-conjugated Phalloidin (10ng/ml final, Sigma) in PBST for 30 minutes to label nuclei and F-actin, respectively, followed by washing 4 more times with 1xPBST.

Image acquisition and data analysis

Using the 20x objectives on an automated Nikon TE300 microscope, triple-channel images from 4 different sites in each well were captured: FITC channel for the level of eGFP expression and information on aggregates within the site; DAPI channel for cell nuclei; and Tritc channel for overall cell morphology. Images from the FITC and DAPI channels in each site were quantified using MetaMorph software (Universal Imaging) to calculate the number, size and signal intensity of the aggregates and determine cell number within the site. For aggregates, images from the FITC channel were segmented based on a pre-determined threshold parameter and their fluorescent intensity was calculated; since the aggregates are highly enriched with eGFP tagged mutant Htt (Httex1-Qp46-eGFP), the level of fluorescent signal from the aggregates is significantly higher than that from the cytoplasm and from background noise, thus allowing their clear identification and quantization by the software (see Fig. 2A). To ensure the accuracy of this automated quantization, we also performed visual scoring and manual quantization for a few selected sites in each plate and confirmed that the manual results were comparable to that from the automated quantization. Similarly, cell numbers in the same site were counted by analyzing

the corresponding DAPI channel images. In general, about 4,000 cells were analyzed for every dsRNA-treated sample. The information on aggregates and cell number was then used to calculate the three parameters for evaluating the effect of dsRNA treatment on aggregates formation: the average number, size and signal intensity of the aggregates, which were further normalized with the cell number in each site. Results from all four sites in the same well were then averaged to assess the aggregation status in this dsRNA-treated well.

Primary screens. Two sets of 63 plates from the DRSC and three sets of two kinase/phosphatase plates from M. Kulkarni (Kulkarni and Perrimon, personal communication), containing 250ng of dsRNA per well, were screened. For each plate screened, the average value and standard deviation (SD) on these three evaluation parameters from the whole plate were also calculated. In the primary screen, those dsRNAs that decreased or increased the aggregates formation by more than 2xSD from the whole-plate average for any of the three evaluation parameters were considered to have a significant effect on aggregates formation and selected as potential candidates.

Secondary screens: See Supplementary Information for detailed description of assays in Secondary screens.

***Drosophila* stocks.** The Httex1p-Q93 and Q48-myc/Flag flies were generously provided by Drs. L. Thompson and J.L. Marsh (STEFFAN *et al.* 2001). The genotype of HD93 flies in the genetic testing is: *GMR-Gal4/+; UAS-Httex1p-Q93*. The following fly *hsp110* alleles showed dosage-dependent genetic interaction with the HD93 flies: *I(3)00082*, *I(3)S031820*, *I(3)S064906*, *I(3)S004112* and *I(3)S0134802*. The following *tra1* alleles were tested and showed dosage-dependent genetic interaction with the HD93 flies: *Nipped-*

A^{NC116} and *Nipped-A*^{NC186}. See Supplementary Information for detailed description of genetic crosses and fly stocks.

Additional information can be found in **Supplementary Information**.

Acknowledgements

We thank the Hereditary Disease Foundation (HDF) for providing mutant Htt plasmids; Drs. L. Thompson, J.L. Marsh, N. Bonini, and M. Feany for providing advice and *Drosophila* stocks; the *Drosophila* RNAi Screening Center (DRSC) for providing technical support; B. Mathey-Prevot for advice and critical reading of the manuscript; M. Markstein and R. Griffin for critical reading of the manuscript; members of the Perrimon lab for assistance, in particular J. Phillips and P. Bradley for microscopy and image analysis, and C. Villalta for fly injection; R.Z. is a Fellow of the Leukemia and Lymphoma Society; S.Z. gratefully acknowledges support in the form of a fellowship from the Harvard Center for Neurodegeneration and Repair (HCNR) as well as the Lieberman Award from the HDF. N. P. is an Investigator of the Howard Hughes Medical Institute.

Author Information The authors declare no competing financial interests. Correspondence and requests for materials should be addressed to N.P. (e-mail: perrimon@receptor.med.harvard.edu) or S.Z. (e-mail: sheng.zhang@uth.tmc.edu).

Legends

Figure 1. Age- and polyQ length-dependent formation of aggregates in *Drosophila*.

(A) Structure of the Htt exon1 (Httex1) constructs used for the studies. eGFP-tagged Httex1 with different lengths of glutamine tract (polyQ) followed by its proline-rich region (P) are under the control of the UAS elements (BRAND and PERRIMON 1993).

(B-P) PolyQ length- and age-dependent formation of aggregates in *Drosophila*.

(B-K) Httex1-Qn-eGFP were expressed in the eye using the eye-specific *GMR-Gal4* driver. Top panels in all the figures show the general eye morphology of adults of different ages, while bottom panels show images of the same eyes under green fluorescent light, with their age and genotype indicated below. Genotypes: (B) *GMR-Gal4/+*, (C-K): *GMR-Gal4/+; UAS-Httex1-Qn-eGFP/+*.

(B) Control of *GMR-Gal4* driver alone at day 2. Note that there is no visible eGFP signal in this eye (bottom panel) in the absence of the *UAS-eGFP* reporter.

(C and D) Adult eyes with Httex1-Q25-eGFP expression. Q25 is found mainly in a diffuse cytoplasmic pattern at both day 2 (C) and day 30 (D). Note that the center bright spots in both eyes and in (E) are not aggregates but rather an optical phenomenon similar to the “deep pseudopupil”, arising from the superimposition of evenly-diffuse GFP signals emitted from the underlying regularly-arranged ommatidia (FRANCESCHINI 1972).

(E-G) Adult eyes with Httex1-Q46-eGFP expression. At day 2 (E, left eye), Httex1-Q46 is found mainly in a diffuse cytoplasmic pattern. As the fly ages,

sporadic aggregates gradually accumulate (F, white arrows) and become prominent by day 30 (G).

(H & I) Adult eyes with Httex1-Q72-eGFP expression. At day 2 (H), Q72 is found mainly in a diffuse cytoplasmic pattern but sporadic aggregates are already visible (H, white arrows). Aggregates become prominent by day 30 (I). (J & K) Adult eyes with Httex1-Q103-eGFP expression. Aggregates already become prominent at day 2 (J) and persist at day 30 (K). Notice also that there is a mild loss of pigment at the posterior of this eye at day 30 (K, white arrowhead in top panel), indicating the degeneration of underlying eye tissues at this stage. In all images, the eyes are oriented as dorsal side is up and anterior to the right.

(L-O) Confocal images of aggregates formation in the brain by the Httex1-Q46-eGFP, which was expressed in the CNS using the pan-neuronal *Elav-Gal4* driver. Genotypes: *Elav-Gal4/+; UAS-Httex1-Q46-eGFP/+*. The protein was distributed evenly and no obvious aggregates were found in the brain at younger age (L and N, day 2), whereas numerous prominent aggregates were present at day 30 (M and O). (N and O) are higher magnification view of regions (the olfactory bulb and the α - and β -lobes of mushroom body) highlighted in (L) and (M), respectively. Note that the images in the younger brain (L and N) were exposed for a longer time to maximize the detection for aggregates.

(P) Confirmation by Western blot of the development of SDS-insoluble aggregates in Httex1-Qn-eGFP flies. Whole protein extracts from adult fly heads were probed with anti-eGFP antibody. Ages and the type of the expressed protein in the examined flies are indicated at the bottom of the panel. Large protein complexes that were retained in the stacking gel, as highlighted, were found in samples from Httex1-Q72, Q103 (lanes 5-7) and aged Q46 flies (lane

4, 30-day-old), but were absent in young Q46 flies (lane 3, 2-day-old) and other control flies (lane 1: flies expressing eGFP alone; lane 2: Httex1-Q23-eGFP; both were 30-day-old).

Figure 2. Imaging-based high-throughput genome-wide RNAi screen for modifiers of aggregates formation in *Drosophila* cells.

(A) Structure of the Httex1-eGFP reporter construct used in the cell-based assay, which are under the control of the copper-inducible (Cu^{++}) *metallothionein* (*met*) promoter.

(B) Confocal images of aggregates formation by Httex1-Qp46-eGFP in *Drosophila* S2 cells. Note that only about 50% of cells developed prominent aggregates, while in the remaining cells the Httex1-Qp46 protein was present diffusively in the cytoplasm. Aggregates were identified by the prominent eGFP signals (green), overall cell morphology using the Tritc-labelled Phalloidin stain (red), and cell nuclei by DAPI (blue).

(C) Automated quantification of aggregates and cell number. Aggregates were revealed by their prominent eGFP signals and the cell nuclei by DAPI staining (left images). Overlaying of computer-simulated objects based on quantification analyses (center images) with their original images revealed significant overlap, demonstrating the accuracy of this quantification method (right images).

(D) Scattered plot comparison of quantification results for two duplicate plates based on the parameters of average aggregates number (left), size (middle) and intensity (right). The circular dashed lines indicate a radius of 2xSD

(standard deviation) for each parameter. Most dsRNAs tested are within the 2XSD range, with the position of CG6603 highlighted (red arrows).

(E) Flow chart for the genome-wide RNAi screen to isolate modifiers of aggregates formation.

Figure 3. Sample images from the RNAi screen.

Examples of images from wells treated with a water control (A), or dsRNAs against eGFP (D), *CG6603* (B, *dhsp110*), *dhdj1* (also known as *dnaj1* or *hsp40*) (C), *lilli* (E) and *smt3* (F). Aggregates were identified by the prominent eGFP signals (green), overall cell morphology using the Tritc-labelled Phalloidin stain (red), and cell nuclei by DAPI (blue).

Figure 4. Functional categorization of aggregation regulators from the screen.

Pie chart representation of candidate genes based upon their Gene Ontology (GO) index biological function or protein domains shows the categories of all 126 hits (A), the 54 suppressors (B) and 72 enhancers (C) that can modulate the formation of mutant Htt aggregates from the screen. “*Enhancer*” is defined as the gene that causes reduced aggregates formation after RNAi-mediated knockdown of target gene expression in the assay. Conversely, “*suppressor*” is defined as the one that causes increased aggregates formation when its expression is knocked down.

Figure 5. *In vivo* modification of the neurodegeneration phenotype associated with a *Drosophila* HD model by Hsp110 and Tra1.

In seven-day old HD93 flies (genotype: *GMR-Gal4/+; UAS-Httex1p Q93/+*) (STEFFAN *et al.* 2001), degeneration is manifested externally by the loss of pigmentation in the posterior of the eye (B), as compared to the control of *GMR-Gal4* eyes (A). By day 30, the degeneration has expanded to encompass the entire eye (E). In a heterozygous *hsp110* (*dhsp110*) mutant background, the degeneration was accelerated and had spread to the entire eye by day 7 (C). Such degeneration was significantly suppressed by co-expression of wild-type *Drosophila* Hsp110 (dHsp110), even at day 30 (F). See also Figure S4 for additional controls for the test. The eye degeneration phenotype of HD93 flies was also significantly accelerated in a heterozygous *tra1* mutant background (D). In all eye images, the anterior side is up and the ventral side is to the left.

Table 1. Summary of aggregation modulators isolated from the screen.

<u>Functional Classes</u>	<u>Number of Modulators</u>	<u>Suppressors</u>	<u>Enhancers</u>
Chaperone	9	6	3
Cytoskeleton/Vesicle/protein trafficking	14	-	14
Jun-N-terminal Kinase (JNK)	5	3	2
Nonsense-mediated mRNA decay (NMD)	4	4	-
Phosphatase/Kinase	6	3	3
Protein Biogenesis	27	8	19
Transcription/Chromatin Modification	17	13	4
Ubiquitin, SUMOylation & Proteasome	14	2	12
Other	8	1	7
Unknown	22	12	10
<i>Total</i>	<i>126</i>	<i>52</i>	<i>74</i>

Table 1 lists the functional classes for the aggregation modulators isolated from the screen (column 1), the total number of modifiers in each functional class (column 2), as well as the number of modifiers in each enhancer and suppressor subset (column 3 and 4). Candidates were categorized based on the “Gene Ontology (GO)” index biological function or protein domains. Please note that in this manuscript, “**Suppressor**” is defined genetically as those candidates that cause an increased formation of aggregates after dsRNA-mediated knockdown of the corresponding candidate gene, and visa versa, “**Enhancer**” is similarly defined as those that cause a decreased formation of aggregates in the assay (also see Fig. 3 and Supplementary Tables S1 and S2 for more details).

Table 2. Aggregation regulators previously identified as toxicity modifiers.

Modifier name	Function	Modification of NDs *	Reference
14-3-3ε	Adaptor protein	PolyQ (SCA1)	CHEN <i>et al.</i> 2003
MADM	Adaptor protein	PolyQ	WU <i>et al.</i> 2005
DnaJ-1	Chaperone (Hsp40)	PolyQ (SCA3)	CHAN <i>et al.</i> 2000.; KAZEMI-ESFARJANI, P., and S. BENZER, 2000
Hsc70-4	Chaperone	PolyQ (SCA3)	CHAN <i>et al.</i> 2000, WARRICK <i>et al.</i> 2000
CG6603	Chaperone Hsp110	PolyQ (HD)	This study
Rpd3	Chromatin modification/Transcription	PolyQ (SCA1)	FERNANDEZ-FUNEZ, P. <i>et al.</i> 2000
Sin3A	Chromatin modification/Transcription	PolyQ (HD)	STEFFAN <i>et al.</i> 2001
Atxain-2	Cytoskeleton	PolyQ (SCA1) & AD (Tau)	SHULMAN <i>et al.</i> 2003
Smt3	SUMO modification	PolyQ (HD)	STEFFAN <i>et al.</i> 2004
Uba2	SUMO modification	PolyQ (SBMA)	CHAN <i>et al.</i> 2002
Tra1 (<i>Nipped-A</i>)	Kinase/transcriptional regulation	PolyQ (HD)	This study
Tor	TOR signaling/autophagy	PolyQ (HD)	RAVIKUMAR <i>et al.</i> 2004
Sec61alpha	Translocon/protein trafficking	PolyQ (HD)	KANUKA <i>et al.</i> 2003
Nup44A **	Nuclear pore component/protein trafficking	PolyQ (SCA1)	FERNANDEZ-FUNEZ, P. <i>et al.</i> 2000

Pros26 **	Proteasome	PolyQ (SCA1)	FERNANDEZ-FUNEZ, P. <i>et al.</i> 2000
Rab1	Vesicle/protein trafficking	PD (a-Synuclein)	COOPER <i>et al.</i> 2006
Tao-1	STE20-related kinase/JNK	AD (Tau)	SHULMAN <i>et al.</i> 2003

Table 2 lists the known toxicity modifiers of neurodegenerative diseases (NDs) that were also isolated as modifiers of aggregates formation from the RNAi screen.

* Modification of NDs: PolyQ: polyglutamine diseases; HD: Huntington's disease; PD: Parkinson's disease; AD: Alzheimer's disease; SCA: Spinocerebellar ataxia type; SBMA: spinalbulbar muscular atrophy.

** Pros26 and Nup44A were not themselves isolated as modifiers of aggregation, but several other components in either the proteasome complex or the nuclear pore complex were isolated in the screen.

REFERENCES

- The Huntington's Disease Collaborative Research Group. 1993. A novel gene containing a trinucleotide repeat that is expanded and unstable on Huntington's disease chromosomes. *Cell* **72**: 971-983.
- ANDREW, S. E., Y. P. GOLDBERG, B. KREMER, H. TELENUS, J. THEILMANN *et al.*, 1993 The relationship between trinucleotide (CAG) repeat length and clinical features of Huntington's disease. *Nat Genet* **4**: 398-403.
- ARRASATE, M., S. MITRA, E. S. SCHWEITZER, M. R. SEGAL and S. FINKBEINER, 2004 Inclusion body formation reduces levels of mutant huntingtin and the risk of neuronal death. *Nature* **431**: 805-810.
- BILEN, J., and N. M. BONINI, 2005 *Drosophila* as a model for human neurodegenerative disease. *Annu Rev Genet* **39**: 153-171.
- BOUTROS, M., A. A. KIGER, S. ARMKNECHT, K. KERR, M. HILD *et al.*, 2004 Genome-wide RNAi analysis of growth and viability in *Drosophila* cells. *Science* **303**: 832-835.
- BRAND, A. H., and N. PERRIMON, 1993 Targeted gene expression as a means of altering cell fates and generating dominant phenotypes. *Development* **118**: 401-415.
- BRUIJN, L. I., T. M. MILLER and D. W. CLEVELAND, 2004 Unraveling the mechanisms involved in motor neuron degeneration in ALS. *Annu Rev Neurosci* **27**: 723-749.
- BUKAU, B., J. WEISSMAN and A. HORWICH, 2006 Molecular chaperones and protein quality control. *Cell* **125**: 443-451.
- CAPLEN, N. J., J. FLEENOR, A. FIRE and R. A. MORGAN, 2000 dsRNA-mediated gene silencing in cultured *Drosophila* cells: a tissue culture model for the analysis of RNA interference. *Gene* **252**: 95-105.
- CAUGHEY, B., and P. T. LANSBURY, 2003 Protofibrils, pores, fibrils, and neurodegeneration: separating the responsible protein aggregates from the innocent bystanders. *Annu Rev Neurosci* **26**: 267-298.
- CHAN, H. Y., J. M. WARRICK, I. ANDRIOLA, D. MERRY and N. M. BONINI, 2002 Genetic modulation of polyglutamine toxicity by protein conjugation pathways in *Drosophila*. *Hum Mol Genet* **11**: 2895-2904.
- CHAN, H. Y., J. M. WARRICK, G. L. GRAY-BOARD, H. L. PAULSON and N. M. BONINI, 2000 Mechanisms of chaperone suppression of polyglutamine disease: selectivity, synergy and modulation of protein solubility in *Drosophila*. *Hum Mol Genet* **9**: 2811-2820.
- CHANG, H. C., M. HULL and I. MELLMAN, 2004 The J-domain protein Rme-8 interacts with Hsc70 to control clathrin-dependent endocytosis in *Drosophila*. *J Cell Biol* **164**: 1055-1064.
- CHANG, H. C., S. L. NEWMYER, M. J. HULL, M. EBERSOLD, S. L. SCHMID *et al.*, 2002 Hsc70 is required for endocytosis and clathrin function in *Drosophila*. *J Cell Biol* **159**: 477-487.
- CHEN, H. K., P. FERNANDEZ-FUNEZ, S. F. ACEVEDO, Y. C. LAM, M. D. KAYTOR *et al.*, 2003 Interaction of Akt-phosphorylated ataxin-1 with 14-3-3 mediates neurodegeneration in spinocerebellar ataxia type 1. *Cell* **113**: 457-468.

- CLEMENS, J. C., C. A. WORBY, N. SIMONSON-LEFF, M. MUDA, T. MAEHAMA *et al.*, 2000 Use of double-stranded RNA interference in *Drosophila* cell lines to dissect signal transduction pathways. *Proc Natl Acad Sci U S A* **97**: 6499-6503.
- COOPER, A. A., A. D. GITLER, A. CASHIKAR, C. M. HAYNES, K. J. HILL *et al.*, 2006 {alpha}-Synuclein Blocks ER-Golgi Traffic and Rab1 Rescues Neuron Loss in Parkinson's Models. *Science*.
- CRAIG, E. A., J. S. WEISSMAN and A. L. HORWICH, 1994 Heat shock proteins and molecular chaperones: mediators of protein conformation and turnover in the cell. *Cell* **78**: 365-372.
- DOUMANIS, J., K. WADA, Y. KINO, A. W. MOORE and N. NUKINA, 2009 RNAi screening in *Drosophila* cells identifies new modifiers of mutant huntingtin aggregation. *PLoS One* **4**: e7275.
- DRAGOVIC, Z., S. A. BROADLEY, Y. SHOMURA, A. BRACHER and F. U. HARTL, 2006 Molecular chaperones of the Hsp110 family act as nucleotide exchange factors of Hsp70s. *Embo J* **25**: 2519-2528.
- EASTON, D. P., Y. KANEKO and J. R. SUBJECK, 2000 The hsp110 and Grp1 70 stress proteins: newly recognized relatives of the Hsp70s. *Cell Stress Chaperones* **5**: 276-290.
- FERNANDEZ-FUNEZ, P., M. L. NINO-ROSALES, B. DE GOUYON, W. C. SHE, J. M. LUCHAK *et al.*, 2000 Identification of genes that modify ataxin-1-induced neurodegeneration. *Nature* **408**: 101-106.
- FRANCESCHINI, N., 1972 Pupil and pseudopupil in the compound eye of *Drosophila*. In *Information Processing in the Visual System of Arthropods* (ed. Wehner, R.). (Springer, Berlin). 1972. pp **75-82**.
- FRIEDMAN, A., and N. PERRIMON, 2007 Genetic screening for signal transduction in the era of network biology. *Cell* **128**: 225-231.
- GARCIA-MATA, R., Z. BEBOK, E. J. SORSCHER and E. S. SZTUL, 1999 Characterization and dynamics of aggresome formation by a cytosolic GFP-chimera. *J Cell Biol* **146**: 1239-1254.
- GATFIELD, D., L. UNTERHOLZNER, F. D. CICCARELLI, P. BORK and E. IZAURRALDE, 2003 Nonsense-mediated mRNA decay in *Drosophila*: at the intersection of the yeast and mammalian pathways. *Embo J* **22**: 3960-3970.
- GUSELLA, J., and M. MACDONALD, 2002 No post-genetics era in human disease research. *Nat Rev Genet* **3**: 72-79.
- HAMAMICHI, S., R. N. RIVAS, A. L. KNIGHT, S. CAO, K. A. CALDWELL *et al.*, 2008 Hypothesis-based RNAi screening identifies neuroprotective genes in a Parkinson's disease model. *Proc Natl Acad Sci U S A* **105**: 728-733.
- ISHIHARA, K., N. YAMAGISHI, Y. SAITO, H. ADACHI, Y. KOBAYASHI *et al.*, 2003 Hsp105alpha suppresses the aggregation of truncated androgen receptor with expanded CAG repeats and cell toxicity. *J Biol Chem* **278**: 25143-25150.
- KANUKA, H., E. KURANAGA, T. HIRATOU, T. IGAKI, B. NELSON *et al.*, 2003 Cytosol-endoplasmic reticulum interplay by Sec61alpha translocon in polyglutamine-mediated neurotoxicity in *Drosophila*. *Proc Natl Acad Sci U S A* **100**: 11723-11728.
- KAZANTSEV, A., E. PREISINGER, A. DRANOVSKY, D. GOLDGABER and D. HOUSMAN, 1999 Insoluble detergent-resistant aggregates form between pathological

- and nonpathological lengths of polyglutamine in mammalian cells. *Proc Natl Acad Sci U S A* **96**: 11404-11409.
- KAZEMI-ESFARJANI, P., and S. BENZER, 2000 Genetic suppression of polyglutamine toxicity in *Drosophila*. *Science* **287**: 1837-1840.
- KULKARNI, M. M., M. BOOKER, S. J. SILVER, A. FRIEDMAN, P. HONG *et al.*, 2006 Evidence of off-target effects associated with long dsRNAs in *Drosophila melanogaster* cell-based assays. *Nat Methods* **3**: 833-838.
- MA, Y., A. CREANGA, L. LUM and P. A. BEACHY, 2006 Prevalence of off-target effects in *Drosophila* RNA interference screens. *Nature* **443**: 359-363.
- MARHOLD, J., TOROK, I., ILIOPOULOS, I., MISHRA, A., DE LORENZO, C., KEMPF, T., SCHMITT, R., MECHLER, B.M., 2000 The TPR-containing Spaghetti protein interacts with Hsp90 and is required for cell survival and differentiation in imaginal discs. *A. Dros. Res. Conf.* **41**.
- MARSH, J. L., and L. M. THOMPSON, 2006 *Drosophila* in the study of neurodegenerative disease. *Neuron* **52**: 169-178.
- MORIMOTO, R. I., 2008 Proteotoxic stress and inducible chaperone networks in neurodegenerative disease and aging. *Genes Dev* **22**: 1427-1438.
- NOLLEN, E. A., S. M. GARCIA, G. VAN HAAFTEN, S. KIM, A. CHAVEZ *et al.*, 2004 Genome-wide RNA interference screen identifies previously undescribed regulators of polyglutamine aggregation. *Proc Natl Acad Sci U S A* **101**: 6403-6408.
- OH, H. J., X. CHEN and J. R. SUBJECK, 1997 Hsp110 protects heat-denatured proteins and confers cellular thermoresistance. *J Biol Chem* **272**: 31636-31640.
- OH, H. J., D. EASTON, M. MURAWSKI, Y. KANEKO and J. R. SUBJECK, 1999 The chaperoning activity of hsp110. Identification of functional domains by use of targeted deletions. *J Biol Chem* **274**: 15712-15718.
- PASINELLI, P., and R. H. BROWN, 2006 Molecular biology of amyotrophic lateral sclerosis: insights from genetics. *Nat Rev Neurosci* **7**: 710-723.
- PENNEY, J. B., JR., J. P. VONSATTEL, M. E. MACDONALD, J. F. GUSELLA and R. H. MYERS, 1997 CAG repeat number governs the development rate of pathology in Huntington's disease. *Ann Neurol* **41**: 689-692.
- POLIER, S., Z. DRAGOVIC, F. U. HARTL and A. BRACHER, 2008 Structural basis for the cooperation of Hsp70 and Hsp110 chaperones in protein folding. *Cell* **133**: 1068-1079.
- PRAHLAD, V., T. CORNELIUS and R. I. MORIMOTO, 2008 Regulation of the cellular heat shock response in *Caenorhabditis elegans* by thermosensory neurons. *Science* **320**: 811-814.
- PRAHLAD, V., and R. I. MORIMOTO, 2009 Integrating the stress response: lessons for neurodegenerative diseases from *C. elegans*. *Trends Cell Biol* **19**: 52-61.
- RAVIKUMAR, B., C. VACHER, Z. BERGER, J. E. DAVIES, S. LUO *et al.*, 2004 Inhibition of mTOR induces autophagy and reduces toxicity of polyglutamine expansions in fly and mouse models of Huntington disease. *Nat Genet* **36**: 585-595.
- RAVIOL, H., H. SADLISH, F. RODRIGUEZ, M. P. MAYER and B. BUKAU, 2006 Chaperone network in the yeast cytosol: Hsp110 is revealed as an Hsp70 nucleotide exchange factor. *Embo J* **25**: 2510-2518.

- ROSS, C. A., and M. A. POIRIER, 2005 Opinion: What is the role of protein aggregation in neurodegeneration? *Nat Rev Mol Cell Biol* **6**: 891-898.
- ROSEN, D. R., T. SIDDIQUE, D. PATTERSON, D. A. FIGLEWICZ, P. SAPP *et al.*, 1993 Mutations in Cu/Zn superoxide dismutase gene are associated with familial amyotrophic lateral sclerosis. *Nature* **362**: 59-62.
- RUBIN, G. M., M. D. YANDELL, J. R. WORTMAN, G. L. GABOR MIKLOS, C. R. NELSON *et al.*, 2000 Comparative genomics of the eukaryotes. *Science* **287**: 2204-2215.
- SCHERZINGER, E., R. LURZ, M. TURMAINE, L. MANGIARINI, B. HOLLENBACH *et al.*, 1997 Huntingtin-encoded polyglutamine expansions form amyloid-like protein aggregates in vitro and in vivo. *Cell* **90**: 549-558.
- SCHERZINGER, E., A. SITTLER, K. SCHWEIGER, V. HEISER, R. LURZ *et al.*, 1999 Self-assembly of polyglutamine-containing huntingtin fragments into amyloid-like fibrils: implications for Huntington's disease pathology. *Proc Natl Acad Sci U S A* **96**: 4604-4609.
- SCHUERMANN, J. P., J. JIANG, J. CUELLAR, O. LLORCA, L. WANG *et al.*, 2008 Structure of the Hsp110:Hsc70 Nucleotide Exchange Machine. *Mol Cell*.
- SHANER, L., H. WEGELE, J. BUCHNER and K. A. MORANO, 2005 The yeast Hsp110 Sse1 functionally interacts with the Hsp70 chaperones Ssa and Ssb. *J Biol Chem* **280**: 41262-41269.
- SHULMAN, J. M., and M. B. FEANY, 2003 Genetic modifiers of tauopathy in *Drosophila*. *Genetics* **165**: 1233-1242.
- SISODIA, S. S., 1998 Nuclear inclusions in glutamine repeat disorders: are they pernicious, coincidental, or beneficial? *Cell* **95**: 1-4.
- SNELL, R. G., J. C. MACMILLAN, J. P. CHEADLE, I. FENTON, L. P. LAZAROU *et al.*, 1993 Relationship between trinucleotide repeat expansion and phenotypic variation in Huntington's disease. *Nat Genet* **4**: 393-397.
- SPILLANTINI, M. G., M. L. SCHMIDT, V. M. LEE, J. Q. TROJANOWSKI, R. JAKES *et al.*, 1997 Alpha-synuclein in Lewy bodies. *Nature* **388**: 839-840.
- STEFFAN, J. S., N. AGRAWAL, J. PALLOS, E. ROCKABRAND, L. C. TROTMAN *et al.*, 2004 SUMO modification of Huntingtin and Huntington's disease pathology. *Science* **304**: 100-104.
- STEFFAN, J. S., L. BODAI, J. PALLOS, M. POELMAN, A. MCCAMPBELL *et al.*, 2001 Histone deacetylase inhibitors arrest polyglutamine-dependent neurodegeneration in *Drosophila*. *Nature* **413**: 739-743.
- VALENCIA-SANCHEZ, M. A., and L. E. MAQUAT, 2004 An enemy within: fly reconnaissance deploys an endonuclease to destroy nonsense-containing mRNA. *Trends Cell Biol* **14**: 594-597.
- VAN HAM, T. J., K. L. THIJSSSEN, R. BREITLING, R. M. HOFSTRA, R. H. PLASTERK *et al.*, 2008 *C. elegans* model identifies genetic modifiers of alpha-synuclein inclusion formation during aging. *PLoS Genet* **4**: e1000027.
- WANG, J., G. W. FARR, D. H. HALL, F. LI, K. FURTAK *et al.*, 2009a An ALS-linked mutant SOD1 produces a locomotor defect associated with aggregation and synaptic dysfunction when expressed in neurons of *Caenorhabditis elegans*. *PLoS Genet* **5**: e1000350.
- WANG, J., G. W. FARR, C. J. ZEISS, D. J. RODRIGUEZ-GIL, J. H. WILSON *et al.*, 2009b Progressive aggregation despite chaperone associations of a

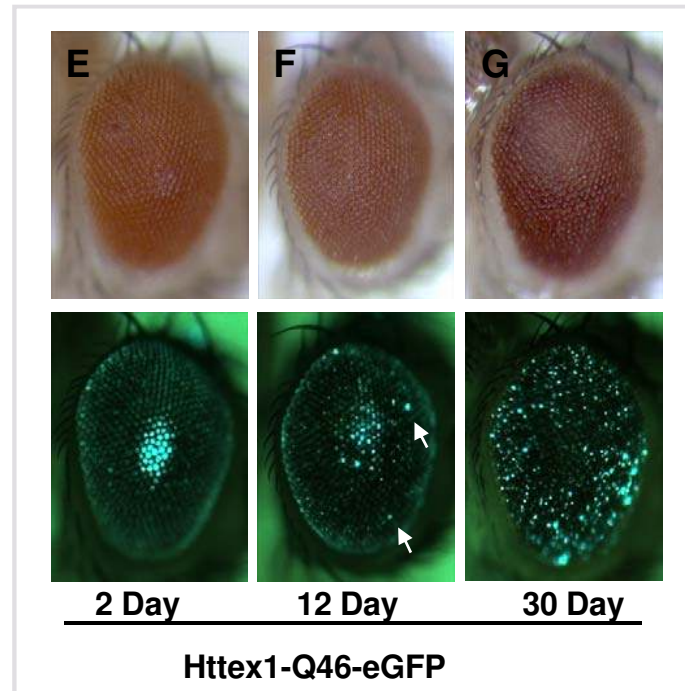
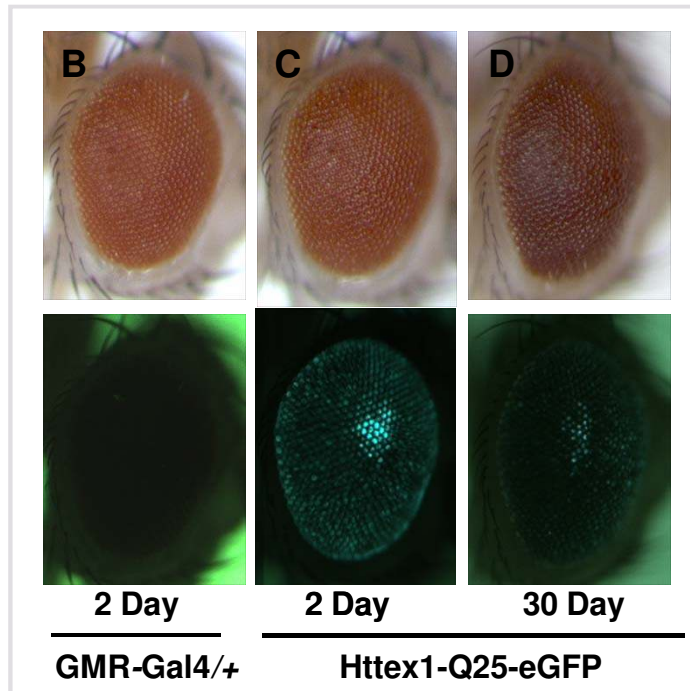
- mutant SOD1-YFP in transgenic mice that develop ALS. Proc Natl Acad Sci U S A **106**: 1392-1397
- WARRICK, J. M., H. Y. CHAN, G. L. GRAY-BOARD, Y. CHAI, H. L. PAULSON *et al.*, 1999 Suppression of polyglutamine-mediated neurodegeneration in *Drosophila* by the molecular chaperone HSP70. Nat Genet **23**: 425-428.
- WESTON, C. R., and R. J. DAVIS, 2002 The JNK signal transduction pathway. Curr Opin Genet Dev **12**: 14-21.
- WHITESSELL, L., and S. L. LINDQUIST, 2005 HSP90 and the chaperoning of cancer. Nat Rev Cancer **5**: 761-772.
- WU, C., FAYAZI, Z., MARION, S., BAO, X., SHERO, M., KAZEMI-ESFARJANI, P., 2005 Modulation of polyglutamine toxicity and aggregation by dMLF and its interaction with 14-3-3zeta and dMADM. A. Dros. Res. Conf. 46 2005 :923B.
- YAM, A. Y., V. ALBANESE, H. T. LIN and J. FRYDMAN, 2005 Hsp110 cooperates with different cytosolic HSP70 systems in a pathway for de novo folding. J Biol Chem **280**: 41252-41261.

Zhang-Figure 1A-G.

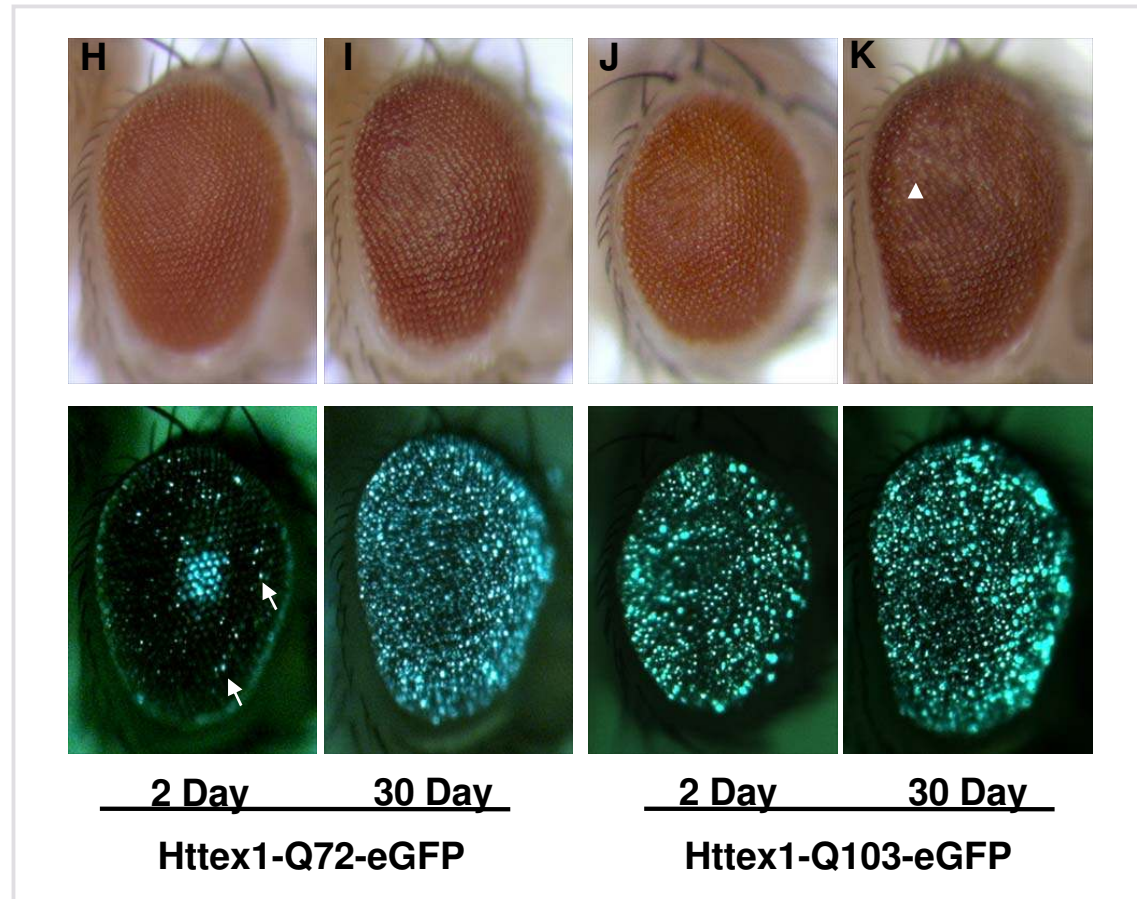
(A)



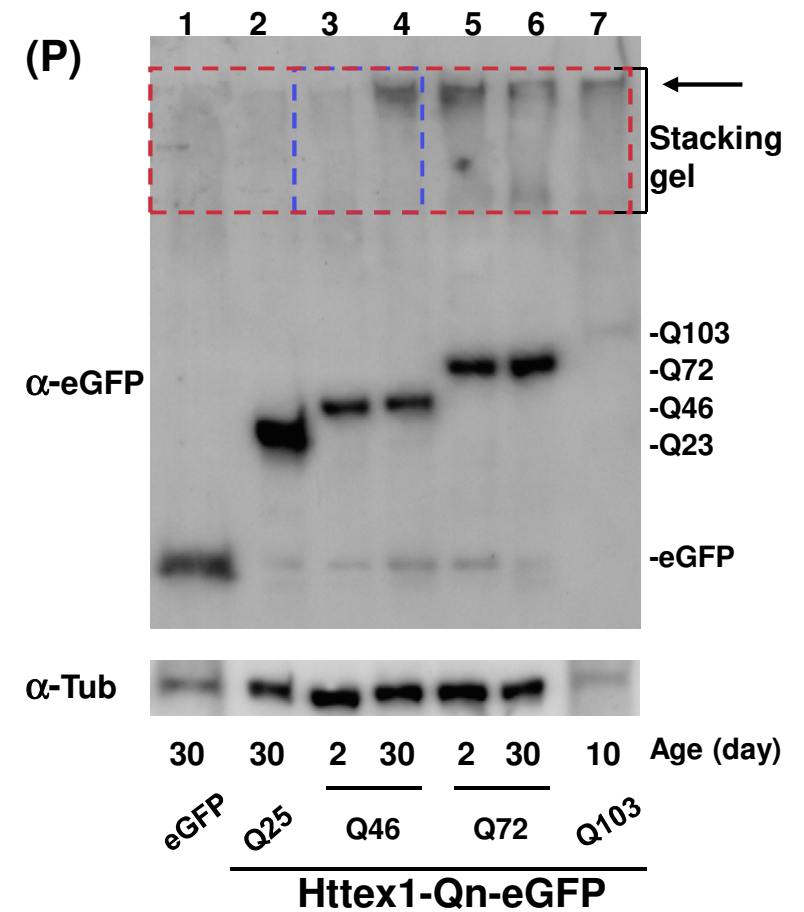
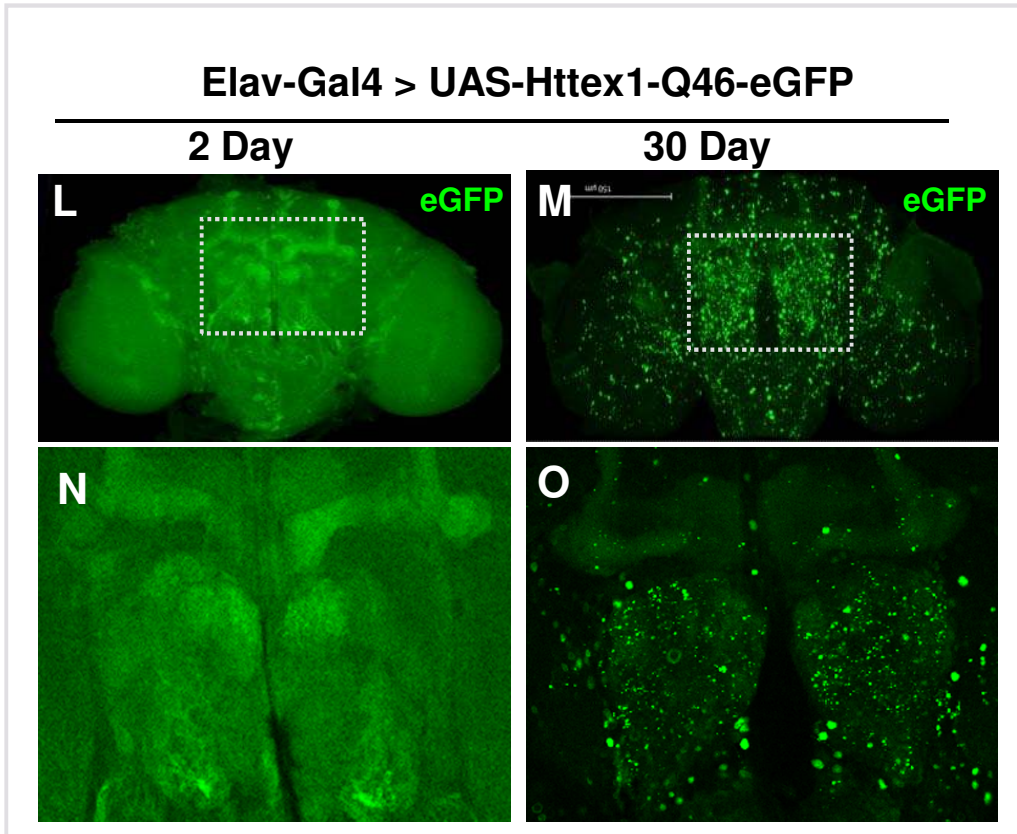
UAS-(Httex1-Qn-eGFP):
n= Q25, Q46, Q72 & Q103



Zhang-Figure 1H-K.



Zhang-Figure 1L-P.



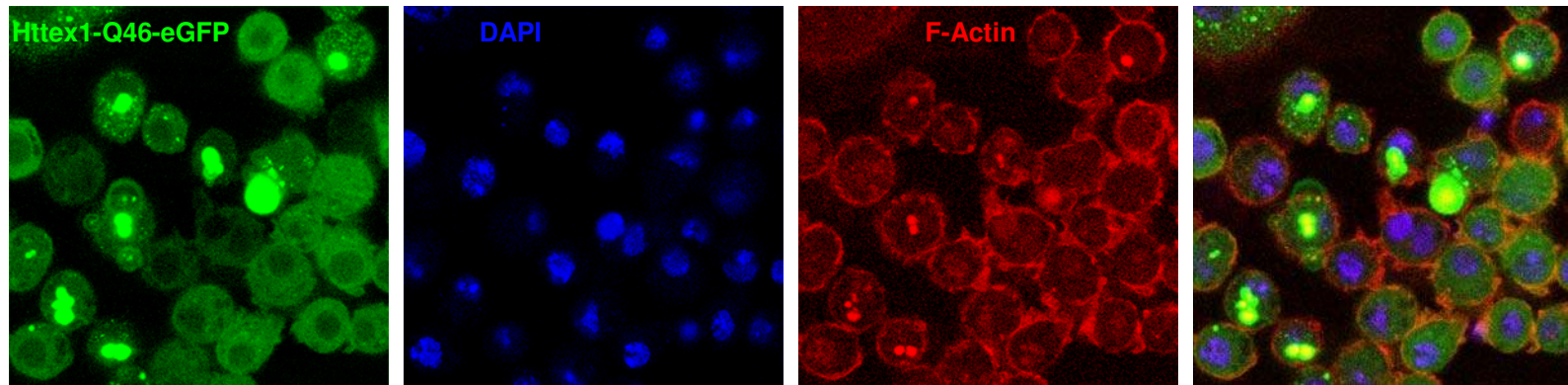
Zhang-Figure 2A, B.

(A)

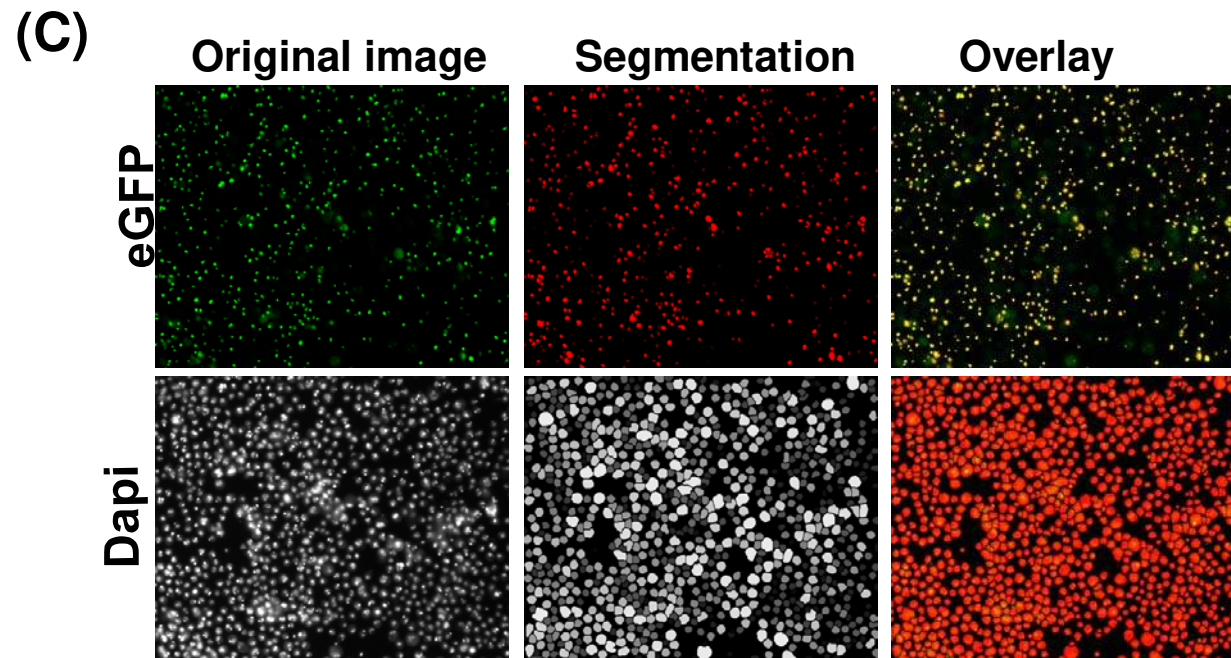


n= Q25, Q46, Q72 & Q103

(B)

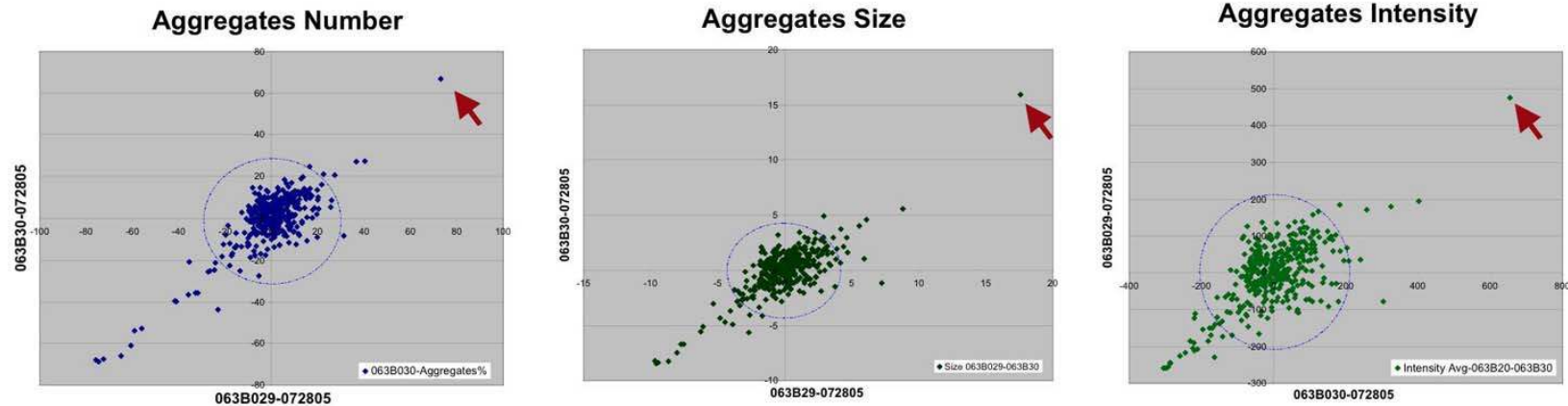


Zhang-Figure 2C.

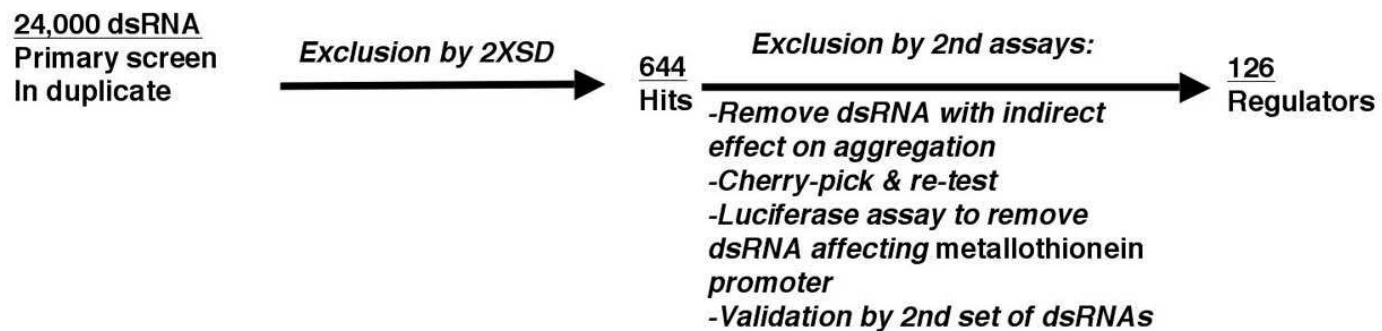


Zhang-Figure 2D, E.

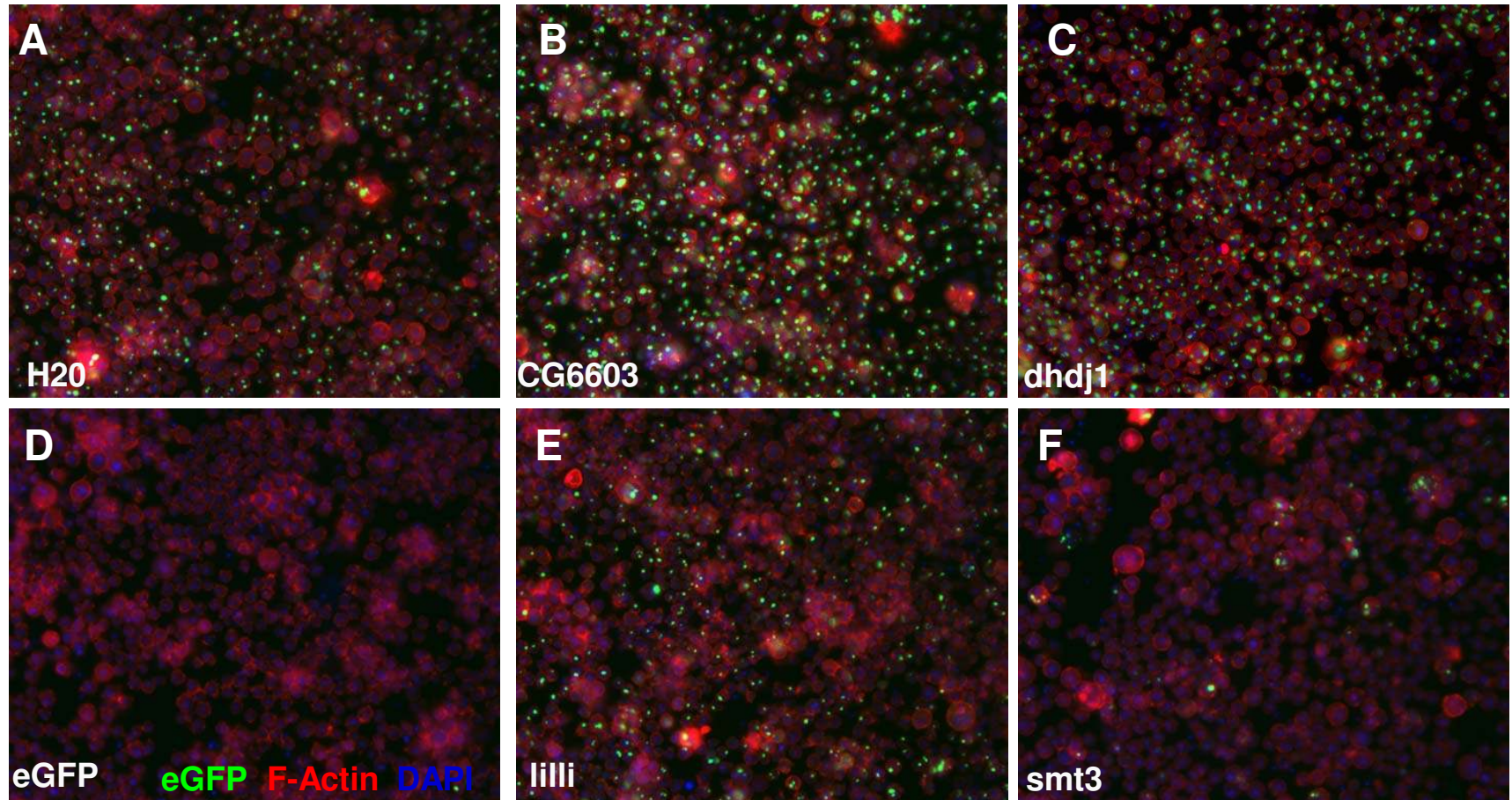
(D)



(E)

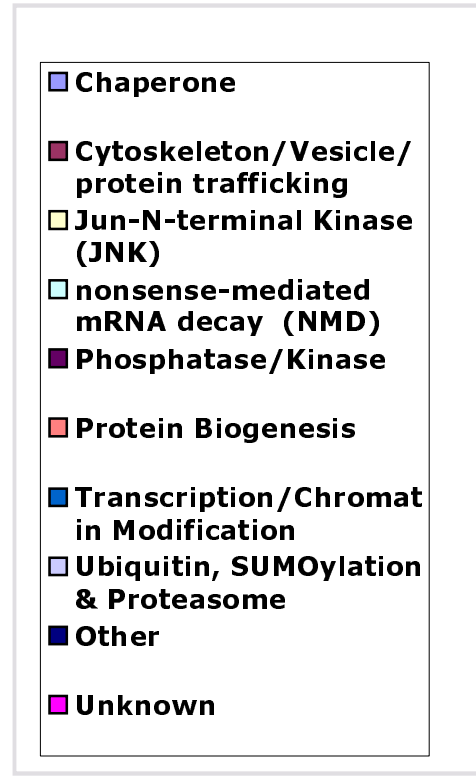
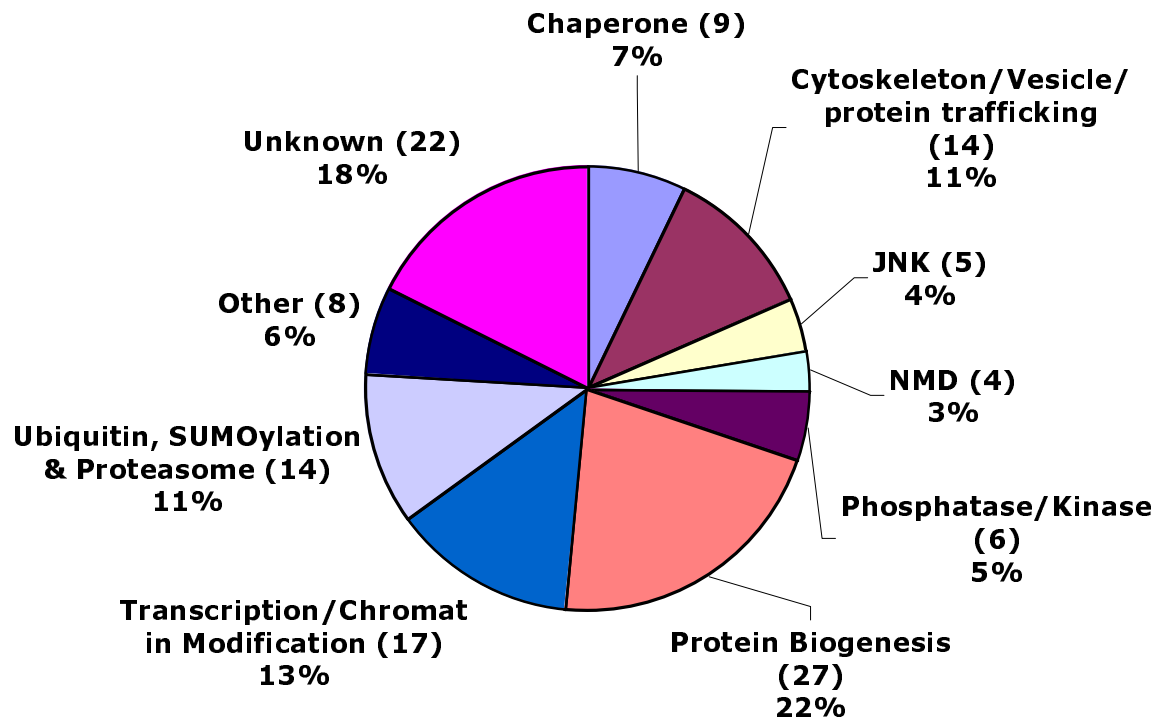


Zhang-Figure 3.



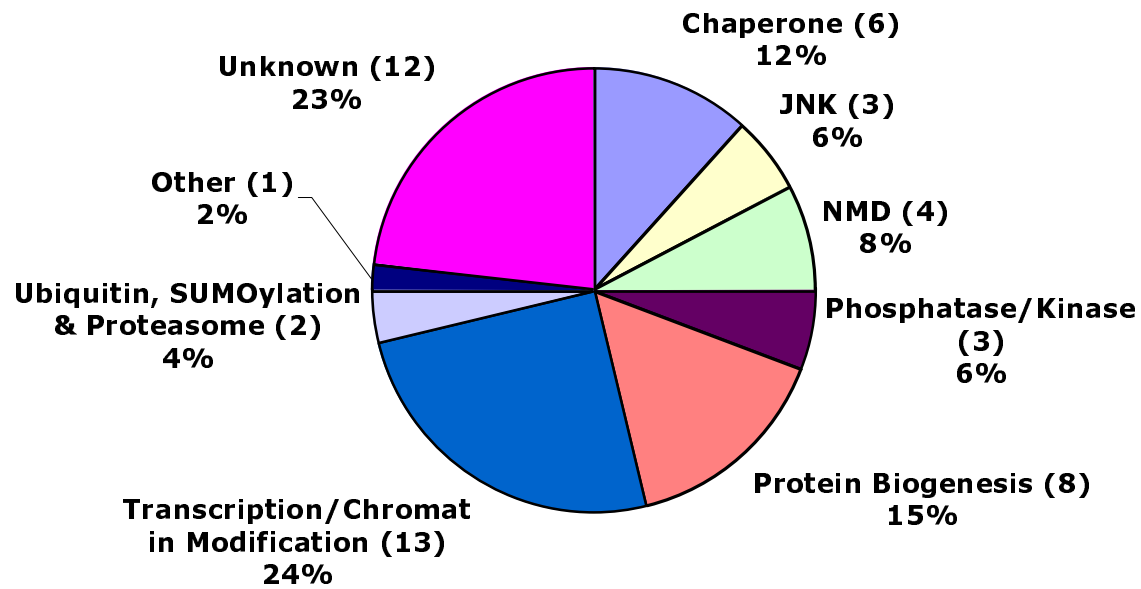
Zhang-Figure 4A.

(A) Aggregation Modifiers (126)



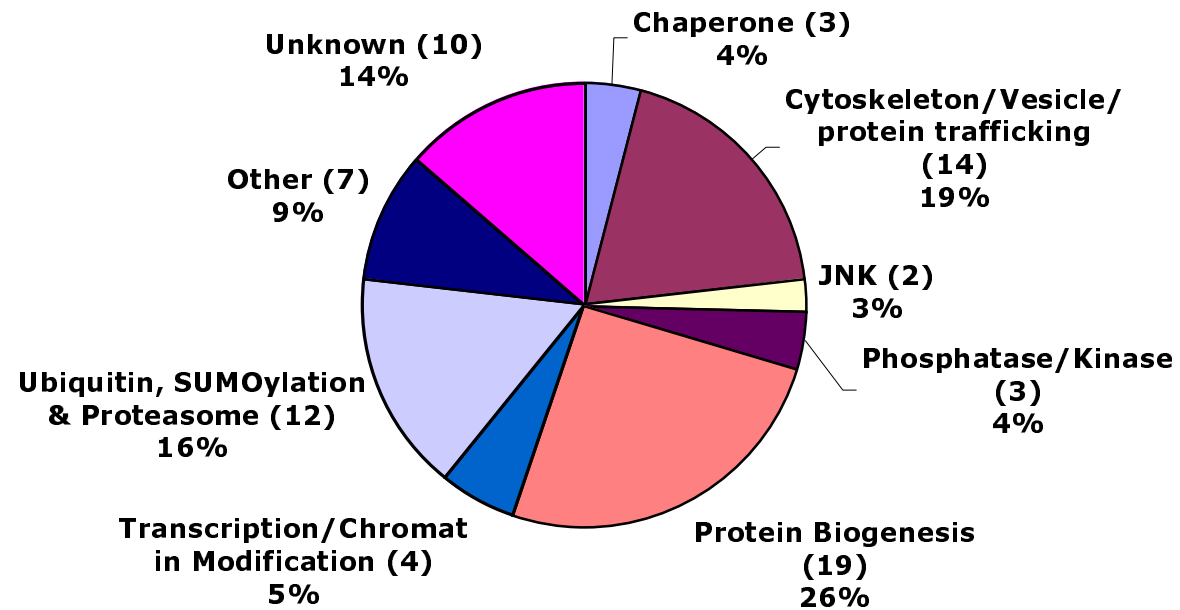
(B)

Suppressors (54)



(C)

Enhancers (72)



Zhang-Figure 5.

